NOAA Technical Report NESDIS 115

IMAGER AND SOUNDER RADIANCE AND PRODUCT VALIDATIONS FOR THE GOES-12 SCIENCE TEST

Washington, D.C.
September 2003

U.S. DEPARTMENT OF COMMERCE
National Oceanic and Atmospheric Administration
National Environmental Satellite, Data, and Information Service

NESDIS 83 Tropical Cyclone Motion Forecasting Using Satellite Water Vapor Imagery. Vernon F. Dvorak and H. Michael Mogil, December 1994.

NESDIS 84 Spurious Semi-Diurnal Variation in the E.R.B.E. Outgoing Longwave Radiation. C. R. Kondragunta and Arnold Gruber, June 1995.

NESDIS 85 Calibration of the Advanced Microwave Sounding Unit-A for NOAA-K. Tsan Mo, June 1995.

NESDIS 86 A Spectral approach to the Forward Problem in GPS Radio Occulation Remote Sensing (Ray Tracing, Assimilation, Tomography). Simon Rosenfeld, July 1996.

NESDIS 87 Proceedings of the International Workshop on Oceanographic Biological and Chemical Data Management. Sponsors Intergovernmental Oceanographic Commission, U.S. National Oceanographic Data Center, European Union MAST Programme, May 1996.

NESDIS 88 Analytical Model of Refraction in a Moist Polytropic Atmosphere for Space and Ground-Based GPS Applications. Simon Rosenfeld, April 1997.

NESDIS 89 A GOES Image Quality Analysis System for the NOAA/NESDIS Satellite Operations Control Center. Donald H. Hillger and Peter J. Celone, December 1997.

NESDIS 90 Automated Satellite-Based Estimates of Precipitation: An Assessment of Accuracy. Michael A. Fortune, June 1998.

NESDIS 91 Aliasing of Satellite Altimeter Data in Exact-Repeat Sampling Mode: Analytic Formulas for the Mid-Point Grid. Chang-Kou Tai, March 1999.

NESDIS 92 Calibration of the Advanced Microwave Sounding Unit-A Radiometers for NOAA-L and NOAA-M. Tsan Mo, May 1999.

NESDIS 93 GOES Imager and Sounder Calibration, Scaling, and Image Quality. Donald W. Hillger, June 1999.

NESDIS 94 MSU Antenna Pattern Data. Tsan Mo, Thomas J. Kleespies, and J. Philip Green, March 2000.

NESDIS 95 Preliminary Findings from the Geostationary Interferometer Observing System Simulation Experiments (OSSE). Bob Aune, Paul Menzel, Jonathan Thom, Gail Bayler, Allen Huang, and Paolo Antonelli, June 2000.

NOAA Technical Report NESDIS 115

IMAGER AND SOUNDER RADIANCE AND PRODUCT VALIDATIONS FOR THE GOES-12 SCIENCE TEST

Donald W. Hillger
NOAA/NESDIS/ORA/RAMMT
Colorado State University
Fort Collins, CO

Timothy J. Schmit
NOAA/NESDIS/ORA/ASPT
University of Wisconsin
Madison, WI

Jaime M. Daniels
NOAA/NESDIS/ORA/CRAD/FPDT
Camp Springs, MD 20746

TABLE OF CONTENTS

Executive Summary

Imager and Sounder Radiance and Product Validations
for the GOES-12 Science Test

Editors:

Donald W. Hillger[1], Timothy J. Schmit[3], and Jaime M. Daniels[5]

Contributors:

A. Scott Bachmeier[4], Gail M. Bayler[4], Daniel E. Bikos[2], Wayne Bresky[6], Jaime M. Daniels[5], Gary P. Ellrod[5], Wayne F. Feltz[4], Mathew M. Gunshor[4], Andy Harris[9], Donald W. Hillger[1], John A. Knaff[2], Eileen M. Maturi[9], Brian C. Motta[2], James P. Nelson III[4], Elaine M. Prins[3], Thomas M. Renkevens[8], Christopher C. Schmidt[4], Timothy J. Schmit[3], Anthony J. Schreiner[4], Justin Sieglaff[4], Gary S. Wade[3], John F. Weaver[1], Michael P. Weinreb[7], and Xiangqian Wu[4]

Affiliations:

[1]ORA/RAMMT (Office of Research and Applications/Regional and Mesoscale Meteorology Team)
[2]CIRA (Cooperative Institute for Research in the Atmosphere)
Colorado State University
Fort Collins CO

[3]ORA/ASPT (Office of Research and Applications/Advanced Satellite Products Team)
[4]CIMSS (Cooperative Institute for Meteorological Satellite Studies)
University of Wisconsin
Madison WI

[5]ORA/FPDT (Office of Research and Applications/Forecast Products Development Team)
[6]Raytheon Information Technology Services Company
Camp Springs MD

[7]ORA/SIT (Office of Research and Applications/Soundings and Instrument Team)
Camp Springs MD

[8]OSDPD/SAB (Office of Satellite Data Processing and Distribution/Satellite Analysis Branch)
Camp Springs MD

[9]ORA/CICS (Office of Research and Applications /Cooperative Institute for Climate Studies)
University of Maryland
College Park MD

Executive Summary of the GOES-12 NOAA Science Test

The Science Test for GOES-12 produced several results and conclusions:

- GOES-12 Imager and Sounder data were collected during the 5-week NOAA Science Test while the satellite was stationed at **90ºW longitude**.

- **Two major changes were implemented with the GOES-12 Imager** compared to previous GOES Imagers:

  1. The elimination of Imager band-5 at 12.0 μm, replaced by a **new band-6 at 13.3 μm.** The GOES-12 Imager will still allow **volcanic ash** to be detected, but with diminished ability, especially for diffuse ash.

  2. **Improved line (or "north-south") resolution**, from 8 km to 4 km, for Imager **water vapor band-3.** The effective element (or "east-west") resolution remains unchanged. The **band-3 spectral width** was also **increased**, moving the **central wavelength from 6.7 μm to 6.5 μm.**

- Imager and Sounder data from GOES-12 are comparable in quality (**noise level**) to that from GOES-8 through GOES-11.

- GOES-12 **Imager** data appear to have slightly increased **detector-to-detector striping** compared to GOES-11. Overall, the Sounder data from GOES-12 are better than from GOES-8. GOES-12 data exhibited **less noise** and **less striping**.

- The GOES-12 Imager **visible spectral response** data showed a similar shift from the specified value to the longer wavelengths. This makes the GOES-12 visible band similar to GOES-11 in its sensitivity to changes in vegetation.

- The **sensitivity** of the GOES-8 (10) **visible band** is about 59% (77%) of the GOES-12 visible band.

- Several improvements were made to the **GOES-12 calibration**. These include invoking the Sounder visible normalization and the Sounder bias calibration mode 2 (which updates the bias factors (intercepts) between space looks based on its correlation with the variation in optics temperature). The Imager and Sounder scan mirror emissivity coefficients were updated.

- The **Imager-to-Imager radiance comparisons** show fair agreement, although the GOES-12 Imager band-3 shows the greatest differences, due to the differing spectral response functions.

- Retrievals of **Total Precipitable Water (TPW)** from the GOES-12 Sounder were improved over those from GOES-8. Derived Product Images (DPIs) of **Lifted Index (LI)** from the GOES-12 Sounder were similar to those from GOES-8.

- Satellite-derived **Sea Surface Temperature (SST)** products were generated from GOES-12 data.

- GOES-12 **fire detection capability** is about the same as GOES-8, but much improved over GOES-10.

- The addition of the **13.3 μm** band has allowed, for the first time on a geostationary **Imager** since GOES-7, the use of the well-known **CO_2 slicing algorithm** to assign heights to viable cloud tracers.

- GOES-12 **cloud-drift winds**, assigned heights from the CO_2 slicing algorithm, validated slightly better against rawinsonde winds than the same GOES-12 cloud-drift winds whose heights were assigned from the H_2O intercept height algorithm.

1.0   Introduction

The Geostationary Operational Environmental Satellite (GOES)-12 was successfully launched on 23 July 2001 and was placed in geostationary orbit at 90ºW. The National Oceanic and Atmospheric Administration (NOAA)/National Environmental Satellite, Data, and Information Service (NESDIS) conducted a 5-week GOES-12 Science Test that began 23 September 2001 and ended on 27 October 2001. The Science Test schedule was integrated within the NESDIS/National Aeronautics and Space Administration (NASA) GOES-12 Post-Launch Test (PLT) schedule. This report describes the NOAA/NESDIS Science Test portion. System performance and operational testing of the spacecraft and instrumentation was performed as part of the PLT. During the Science Test, GOES-12 was operated in a special test mode, where the default schedule involved continuous imaging of the continental United States at 5-minute intervals. Numerous other scan schedules and sectors were constructed and used for both the Imager and the Sounder.

Several goals were established for the GOES-12 Science Test:

- Investigate the impact of the loss of the 12 µm Imager band-5 (and the addition of the 13.3 µm band-6) on both current and new Imager products. Investigate how the Imager water vapor band-3 (6.5 µm) compares to the previous Imager band-3 (6.7 µm).

- Investigate and quantify/characterize the quality of the GOES-12 measurements. This was accomplished by comparing GOES-12 data to measurements from other satellites and by performing noise and striping analyses.

- Generate and validate Imager and Sounder products from GOES-12 measurements. These products include temperature/water vapor retrievals, total precipitable water, lifted index, cloud-top pressure, satellite-derived winds, sea surface temperatures, biomass burning and volcanic ash analyses. Validation of these products was accomplished by comparing these products to products generated from other satellites or by comparing them to radiosondes and ground-based instruments.

- Investigate the utility of nearly continuous rapid scan Imager and Sounder imagery for improving severe weather forecasts.

- Archive GOES-12 GVAR data stream and ancillary data for use in retrospective studies.

This report documents results from these various activities undertaken by NESDIS and its Cooperative Institutes during this test period. Organizations which participated in these GOES-12 Science Test activities included the: NOAA/NESDIS Office of Research and Applications (ORA); NOAA/NESDIS Office of Satellite Data Processing and Distribution (OSDPD); Cooperative Institute for Meteorological Satellite Studies (CIMSS); Cooperative Institute for Research in the Atmosphere (CIRA); and NOAA/NESDIS Satellite Analysis Branch (SAB).

GOES-12 data was received via direct downlink at the following sites: (1) CIRA, Colorado State University, Fort Collins CO; (2) Space Science and Engineering Center (SSEC), University of

Wisconsin, Madison WI; and (3) NESDIS, Suitland/Camp Springs MD. Each site ingested the data and made it available on its own internal network in McIDAS (Man computer Interactive Data Access System) format. The Regional and Mesoscale Meteorology (RAMM) team of NESDIS and CIRA made the GOES-12 imagery available over the internet via the RAMSDIS Online homepage. Image and product loops were also made available on the CIMSS Web pages.

The GOES-12 Imager and Sounder data transmitted during the Science Test were archived (in various formats and to varying degrees) at several sites: (1) CIRA, Colorado State University, Fort Collins CO; (2) SSEC, University of Wisconsin, Madison WI; and (3) NESDIS Forecast Products Development Team (FPDT). The FPDT made a best effort to archive all of the Imager and Sounder data ingested, as well as ancillary data (model data, hourly surface observations, radiosonde data) during the Science Test period. Both CIRA and SSEC archived the entire GVAR data stream.

2.0   Satellite Schedules and Sectors

A total of six schedules involving numerous predefined Imager and Sounder sectors were constructed for the GOES-12 Science Test. The choice of Imager and Sounder sectors was a result of input from the various research and development groups participating in the Science Test. These schedules are similar to those run during the GOES-11 PLT (Daniels et al. 2001). Thanks to dedicated support provided by the NESDIS/Satellite Operations Control Center (SOCC), a significant amount of flexibility existed with respect to switching and activating the schedules. The ease with which the schedules could be activated was important for capturing significant weather phenomena of varying scales during the Science Test period. For example, a different schedule could be invoked by SOCC with two hours prior notification.

A brief summary of the six schedules is provided in Table 2.1. In the default C1RAP schedule, the Imager performed continuous 5-min scans over the continental United States (conus). For the Sounder, the default scan was the East conus view. The C2SRSO schedule was prepared to provide a limited ability to call up Super Rapid Scan Operations (SRSO) during the test period.

Table 2.1: Summary of Schedules/Sectors for the GOES-12 Science Test.

Test Schedule	Imager		Sounder	
	Time Interval	Sector / Area	Time Interval	Sector / Area
C1RAP	Continuous 5 min	Conus, Atlantic Hurricane, Pacific Hurricane, Central/S. America	26-min sector every 30 min	East conus, West conus, Gulf of Mexico, Tropical Pacific, Caribbean, Central/S. America, Volcano, East limb, West limb
C2SRSO	Continuous 1 min, plus 5 min conus every hour	Selected by center point	26-min sector every 30 min	Same as C1 above

C3	Continuous 5 min	Conus	9 min	Colorado, Oklahoma, or Hurricane 10, 11, or 12
C4	Continuous 8 min	South America	1 hour	South America
C5	Continuous emulation of GOES-east operations	GOES-east	Continuous emulation of GOES-east operations	GOES-east
C6	Continuous 2 min, plus conus every hour	Gulf of Mexico	26-min sector every 30 min	Same as C1 above

The daily implementation of the various schedules during the entire Science Test is presented in Table 2.2. Full flexibility in the GOES-12 schedule was in effect during most of the Science Test period, 23 September to 27 October 2001, except for a few days at the beginning when Image Navigation and Registration (INR) specification testing required implementation of the C1RAP schedule.

Table 2.2: Daily Implementation of GOES-12 Science Test Schedules.

Date (Staring Time: 1800 UTC)	Imager	Sounder	Notes
September 23	C1RAP conus	East conus	First Day of Science Test
September 24	C5	East conus	GOES-8 Emulation
September 25	C1RAP conus	East conus	Pre-arranged tests
September 26	C1RAP conus	East conus	Pre-arranged tests
September 27	C1RAP conus	East conus	Pre-arranged tests
September 28	C1RAP conus	East conus	Pre-arranged tests
September 29	C1RAP conus	East conus	Pre-arranged tests
September 30	C1RAP conus	East conus	
October 01	C5	East conus	GOES-8 Emulation
October 02	C5	East conus	GOES-8 Emulation
October 03	C2SRSO at 15°N 110°W through 0043 UTC; then C1RAP Pacific Hurricane	Tropical Pacific	Tropical Storm Lorena
October 04	C1RAP Hurricane Atlantic	Caribbean	
October 05	C1RAP Hurricane Atlantic	Caribbean	
October 06	C1RAP Hurricane Atlantic	Caribbean	Saturday
October 07	C1RAP Hurricane Atlantic	Caribbean	Sunday
October 08	C1RAP Hurricane Atlantic	Caribbean	Columbus Day
October 09	C2SRSO at 40°N 99°W through 0043 UTC; then	East conus	Severe weather in Central Plains

	C1RAP conus		
October 10	C5	C5 (East conus)	GOES-8 Emulation
October 11	C5 through 0543 UTC; then C2SRSO at 32°N 95°W	East conus	Severe weather in Gulf States
October 12	C2SRSO at 32°N 95°W through 0543 UTC; then C1RAP conus	East conus	Severe weather in Gulf States
October 13	C1RAP conus	East conus	Saturday
October 14	C1RAP conus	East conus	Sunday
October 15	C1RAP conus	East conus	TS Karen – Nova Scotia
October 16	C1RAP conus	C1 East limb through 0600 UTC C1 West limb from 0600 UTC	Sounder Limb Scans
October 17	C5	C5 East conus	Tranquil Weather
October 18	C1RAP conus	C1 West limb through 0600 UTC C1 East limb from 0600 UTC	Sounder Limb Scans
October 19	C1RAP conus	East conus	Friday
October 20	C1RAP conus	East conus	Saturday
October 21	C1RAP conus	East conus	Sunday
October 22	C1 Pacific Hurricane	East conus*	*Pacific Hurricane request somehow did not make it
October 23	C3 conus	C3 Oklahoma	Rapid Sounder Scans over Oklahoma
October 24	C2SRSO centered at 40°N/83°W	East conus	Severe weather in Midwest
October 25	C2SRSO centered at 48°N/79°W	East conus	Severe weather in New England, Large Low north of Great Lakes, Lake Effect Snow
October 26	C1RAP conus	East conus	
October 27	C1RAP conus	East conus	Last Day of Science Test

3.0 Changes to GOES-12 (and successive GOES) Imagers compared to previous GOES-8 through GOES-11

The differences between bands utilized by the two versions of the GOES Imager (Schmit et al. 2001) are explained in Table 3.1. Both versions have five bands. The Imager on GOES-8 through GOES-11 contains bands 1 through 5. The Imager on GOES-12 (and future GOES) contains bands 1 through 4 and band-6.

Table 3.1: GOES Imager bands.

GOES Imager Band	Wavelength Range (µm)	Central Wavelength (µm)	Meteorological Objective
1	0.55 to 0.75	0.65	Cloud cover and surface features during the day
2	3.8 to 4.0	3.9	Low cloud/fog and fire detection
3	6.5 to 7.0 5.8 to 7.3	6.75 **(GOES-8/11)** 6.48 **(GOES-12)**	Upper-level water vapor
4	10.2 to 11.2	10.7	Surface or cloud top temperature
5	11.5 to 12.5	12.0 **(GOES-8/11)**	Surface or cloud top temperature and low-level water vapor
6	12.9 to 13.7	13.3 **(GOES-12)**	CO_2 band: Cloud detection

Changes to the GOES-12 Imager compared to previous GOES (8 through 11) include:

- A new band-6 at 13.3 µm at 8 km spatial (line) resolution at nadir. This band replaces band-5 at 12.0 µm.

- The water vapor (band-3) is now available at an improved 4 km spatial (line) resolution, compared to the 8 km (line) resolution on current GOES. (Both bands are collected at an over-sampled 2.3 km element resolution.) The spectral response of the water vapor band was also shifted slightly and broadened. See Table 3.2.

Table 3.2: GOES Imager spatial resolution characteristics.
(GOES-8/11 values are from Menzel and Purdom 1994)

GOES Imager Band	GOES-8/11		GOES-12/N	
	IGFOV* (km)	SSR** (km)	IGFOV* (km)	SSR** (km)
1	1.0 x 1.0	0.57 x 1.0	1.0 x 1.0	0.57 x 1.0
2	4.0 x 4.0	2.3 x 4.0	4.0 x 4.0	2.3 x 4.0
3	8.0 x 8.0	2.3 x 8.0	4.0 x 4.0	2.3 x 4.0
4	4.0 x 4.0	2.3 x 4.0	4.0 x 4.0	2.3 x 4.0
5	4.0 x 4.0	2.3 x 4.0	No band	No band
6	No band	No band	8.0 x 8.0	2.3 x 8.0

*IGFOV = Instantaneous Geometric Field Of View (line x element) at sub-satellite point
**SSR = Sampled Subpoint Resolution (line x element) due to east-west over-sampling

Examples of both of these new features of the Imager are shown and explained by Hillger (2002) and at: http://www.cira.colostate.edu/ramm/picoday/011119/011119.html

4.0 GOES Data Quality

4.1 First Images

4.1.1 Visible

The first full-disk visible image from the GOES-12 Imager occurred on 17 August 2001 at 1800 UTC and is shown in Figure 4.1. This image was captured at SSEC and can also be seen at: http://www.ssec.wisc.edu/data/goes12/. Full spatial resolution data showed good integrity. GOES-12 images were compared to GOES-8 and GOES-10 visible images from approximately the same times. As expected, degradation of the visible bands in the GOES-8 and GOES-10 Imagers and Sounders was apparent.
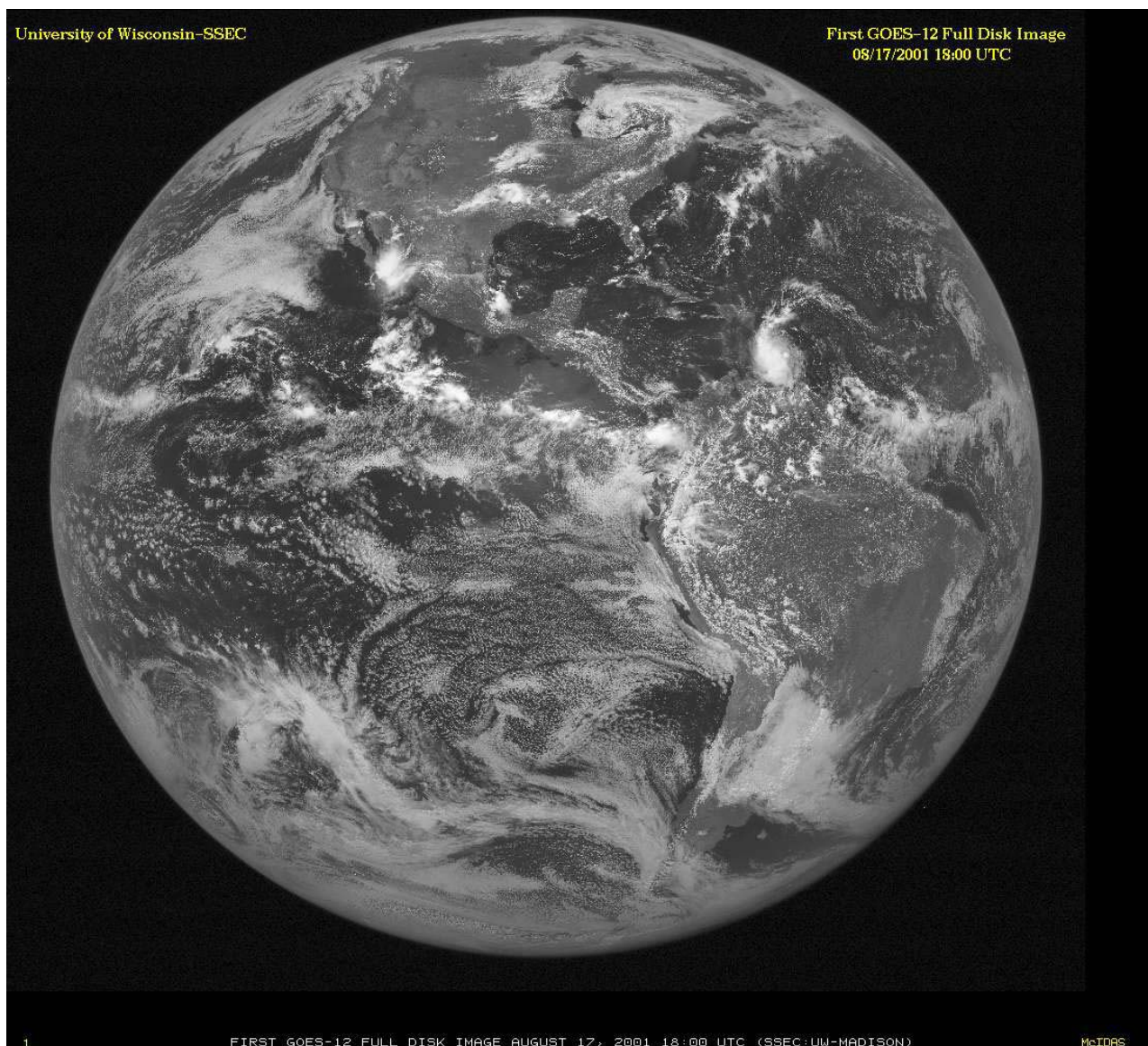
Figure 4.1: The first visible image from the GOES-12 Imager occurred on 17 August 2001 at 1800 UTC.

4.1.2 *Infrared*

One of the first full-disk infrared images from the GOES-12 Imager occurred on 17 September 2001 at 1800 UTC. Full-disk images for the infrared window band (band-4, 10.7 μm) and the water vapor band (band-3, 6.5 μm) are shown in Figures 4.2 and 4.3, respectively. These can also be seen at: http://www.ssec.wisc.edu/data/goes12/.
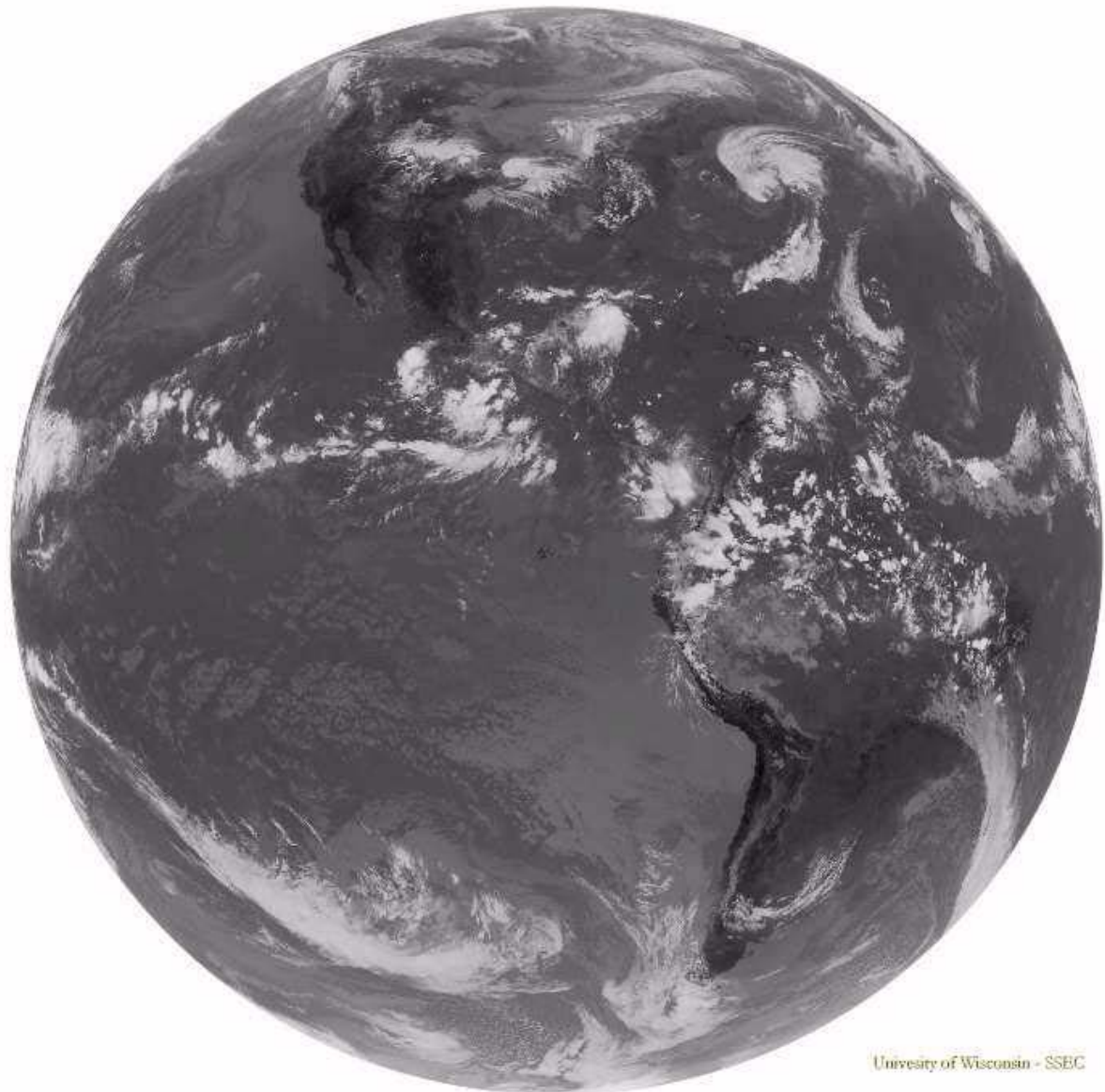
Figure 4.2: GOES-12 full-disk image for the infrared window band (band-4, 10.7 μm).

Figure 4.3: GOES-12 full-disk image for the water vapor band (band-3, 6.5 μm).

4.1.3 Sounder

The first visible band image for the GOES-12 Sounder occurred on 30 August 2001 at 1631 UTC. This image is compared to a GOES-8 visible image from approximately the same time at: http://cimss.ssec.wisc.edu/goes/g12_report/G12SOUNDERVIS_30AUG01_TITLE.jpg. Degradation in the GOES-8 Sounder is apparent. Note that GOES-12 visible data were not yet normalized, as GOES-8 data are, hence the striping in the GOES-12 image. Despite this, it is considerably brighter than the GOES-8 image.

4.2 Spectral Response Functions

4.2.1 Imager

The GOES spectral response functions for any of the GOES-I/M series Imagers can be found at: http://www.oso.noaa.gov/goes/goes-calibration/goes-imager-srfs.htm and are plotted in Figure 4.4. Information about the GOES calibration can be found in Weinreb et al. 1997.
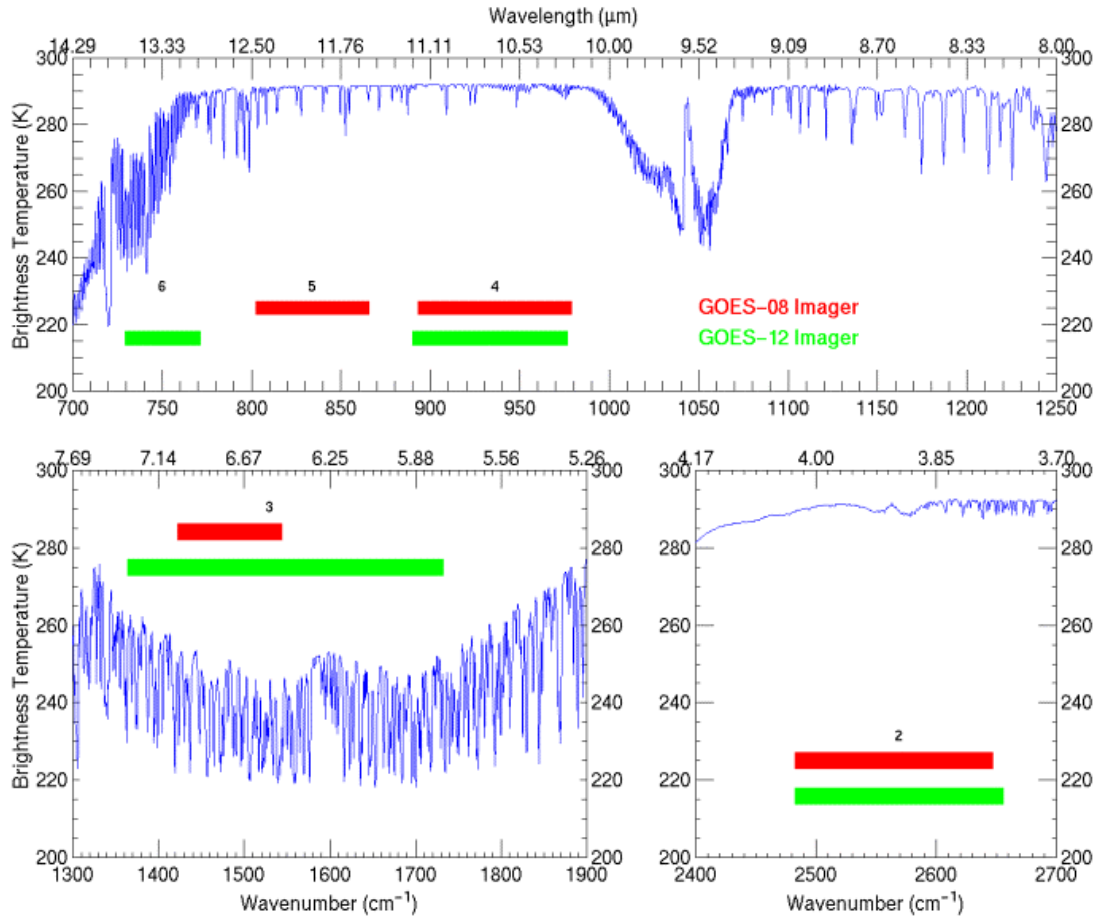
Figure 4.4: Locations of the four GOES-12 Imager IR spectral response functions, superimposed over a high-resolution earth-emitted spectrum. Absorption due to carbon dioxide (CO_2), water vapor (H_2O), and other gases are evident in the high-spectral resolution earth-emitted spectrum.

4.2.2 Sounder

The GOES spectral response functions for any of the GOES-I/M series Imagers can be found at: http://www.oso.noaa.gov/goes/goes-calibration/goes-sounder-srfs.htm.   Locations of the 18 infrared GOES-12 Sounder band spectral response functions, superimposed over a high-resolution earth-emitted spectrum, are shown in Figure 4.5. The band selection is unchanged from previous GOES Sounders (Schmit et al. 2002). As before, the carbon dioxide (CO_2), ozone (O_3), and water vapor (H_2O) absorption bands are indicated in the high-spectral resolution earth-emitted spectrum.
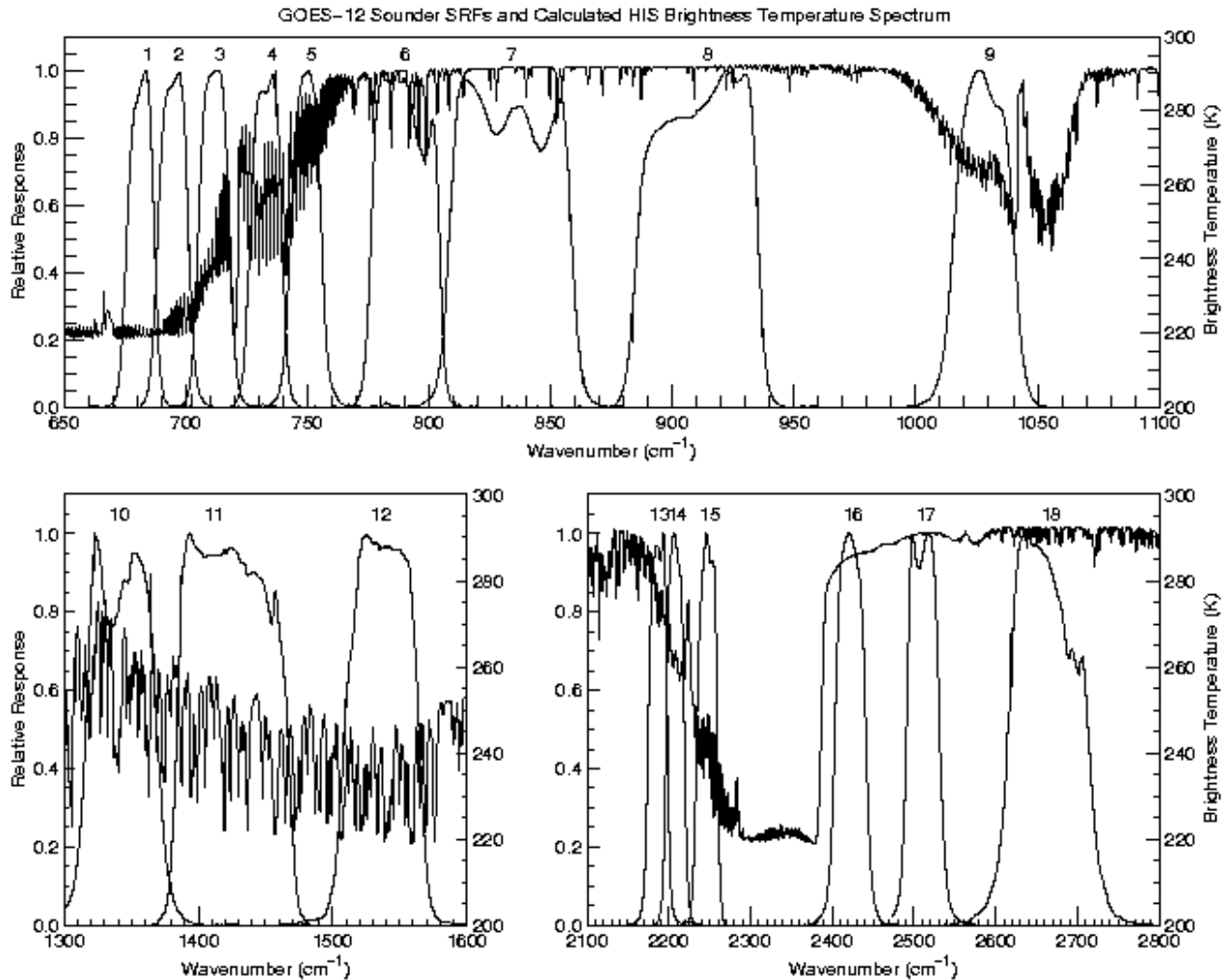
Figure 4.5: Locations of the GOES-12 Sounder IR average spectral response functions super-imposed over a high-resolution earth-emitted spectrum. The central wavenumbers (wavelengths) of the spectral bands range from 680 cm^{-1} (14.7 μm) to 2667 cm^{-1} (3.75 μm) (Menzel et al. 1998).

4.3   Random Noise Estimates

Band noise estimates for the GOES-12 Imager and Sounder instruments were computed using two different approaches. In the first approach, the band noise values were determined by calculating the variance of radiance values in a space look scene. The second approach involved performing a spatial structure analysis (Hillger and Vonder Haar, 1988). Both approaches yielded nearly identical band noise estimates and are presented below.

4.3.1   Imager

Full-disk images for the Imager provided space views and allowed noise values to be determined. Preliminary noise values for the GOES-12 Imager from 5 November 2001 at 2100 UTC were similar to those for GOES-11 as in Table 4.1.

Table 4.1: Preliminary Noise Estimates for GOES-12 for 5 November 2001 at 2100 UTC Compared to Preliminary Noise Values for GOES-11.

Imager Band	Central Wavelength (μm)	GOES-12	GOES-11
		mW/(m^2·sr·cm^{-1})	
2	3.9	0.008	0.005
3	6.5 / 6.7	0.02	0.03
4	10.7	0.17	0.12
5	12.0	No band	0.31
6	13.3	0.32	No band

Noise is estimated using spatial structure analysis on a 50-line by 100-element space-view portion of the images. Structure analysis compares adjacent Fields-Of-View (FOVs) to determine the random component of the signal in the images. The analysis was performed on 15-minute GOES-12 imagery over a 6-h period from 26 November 2001 [Julian day 330] 0915 UTC through 1515 UTC. Results for GOES-12 are presented in Table 4.2, with equivalent values for GOES-11 given for comparison.

Table 4.2: GOES-12 Imager Noise Compared to GOES-11.

Imager Band	Central Wavelength (μm)	GOES-12	GOES-11	GOES-12	GOES-11
		(GVAR count, 10-bit, 0-1023)		(K @ 300 K, except band-3 @ 230 K)	
2	3.9	1.1	1.2	0.13	0.14
3	6.5 / 6.7	0.85	1.2	0.15	0.22
4	10.7	1.0	0.7	0.11	0.08
5	12.0	No band	1.8	No band	0.20
6	13.3	1.8	No band	0.19	No band

GOES-12 noise is compared to the rest of the GOES series (GOES-8 through GOES-11) in Table 4.3. GOES-12 noise levels compare well with those from the other satellites.

Table 4.3: Summary of the noise (in temperature units) for GOES-8 through GOES-12 Imager bands. The specification (SPEC) noise values are also listed.

Imager Band	Central Wavelength (µm)	GOES-12	GOES-11	GOES-10	GOES-9	GOES-8	SPEC
		(K @ 300 K, except band-3 @ 230 K)					
2	3.9	0.13	0.14	0.17	0.08	0.16	1.40
3	6.5 / 6.7	0.15	0.22	0.09	0.15	0.27	1.00
4	10.7	0.11	0.08	0.20	0.07	0.12	0.35
5	12.0	No band	0.20	0.24	0.14	0.20	0.35
6	13.3	0.19	No band	No band	No band	No band	0.32

4.3.2   Sounder

Special GOES-12 Sounder sectors that include space views allow noise values to be determined by the scatter of radiance values looking at uniform space. Preliminary indications from 19 October at 1316 UTC show that GOES-12 appears to be within specification for most bands. The line plot in Figure 4.6 comparing GOES-8 and GOES-12 to SPECS illustrates the improvement over GOES-8 noise values in the shortwave and longwave infrared. The GOES-12 signal to noise values (in radiance units) compared well with those from other satellites.
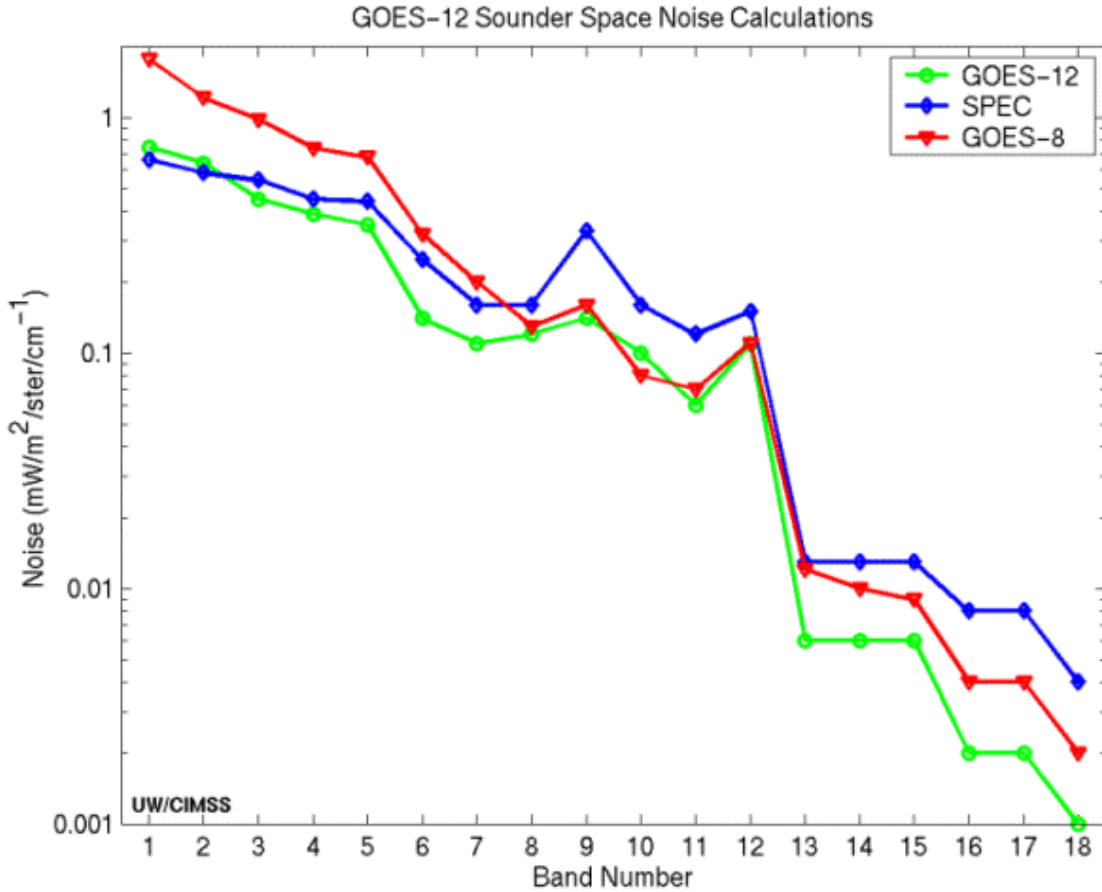
Figure 4.6: GOES-12 Sounder noise values (in radiance units) compared to those from GOES-8. The specification noise values for the GOES Sounder bands are also included for comparison purposes.

Structure analysis was performed on half-hourly space-view measurements acquired over a 24-h period: 16 October 2001 [Julian day 289] 1816 UTC through 17 October 2001 [Julian day 290] 1716 UTC. East-limb, west-limb, and limb-average values are presented and compared to CIMSS analysis values in Table 4.4.

Table 4.4: GOES-12 Sounder Noise Levels.

Sounder Band	Central Wavelength (μm)	East Limb	West Limb	Limb Average	Limb Average	CIMSS Analysis
		13-bit GVAR counts (0-8191)			(mW/(m^2·sr·cm^{-1}))	
1	14.71	51.2	51.3	51.2	0.77	0.75
2	14.37	41.2	41.5	41.3	0.61	0.64
3	14.06	26.9	27.5	27.2	0.45	0.45
4	13.64	18.9	19.0	19.0	0.39	0.39
5	13.37	15.4	15.6	15.5	0.34	0.35
6	12.66	5.92	5.90	5.91	0.14	0.14
7	12.02	4.18	4.15	4.17	0.11	0.11
8	11.03	4.21	4.66	4.44	0.11	0.12
9	9.71	7.34	7.78	7.56	0.14	0.14
10	7.43	13.8	14.2	14.0	0.099	0.10
11	7.02	13.7	14.2	14.0	0.059	0.06
12	6.51	37.5	38.2	37.9	0.11	0.11
13	4.57	7.21	7.81	7.51	0.0062	0.006
14	4.52	10.3	11.7	11.0	0.0062	0.006
15	4.46	20.3	22.9	21.6	0.0066	0.006
16	4.13	3.19	3.29	3.24	0.0024	0.002
17	3.98	3.24	3.55	3.40	0.0022	0.002
18	3.74	2.21	2.35	2.28	0.00094	0.001

GOES-12 noise is compared to the rest of the GOES series (GOES-8 through GOES-11) in Table 4.5. GOES-12 noise levels compare well with those from the other satellites.

Table 4.5: Summary of the noise for GOES-8 through GOES-12 Sounder bands. The specification (SPEC) values are also listed.

Sounder Band	Central Wavelength (µm)	GOES-12	GOES-11	GOES-10	GOES-9	GOES-8	SPEC

Sounder Band	Central Wavelength (µm)	GOES-12	GOES-11	GOES-10	GOES-9	GOES-8	SPEC
		$(mW/(m^2 \cdot sr \cdot cm^{-1}))$					
1	14.70	0.77	0.67	0.71	1.16	1.76	0.66
2	14.40	0.61	0.51	0.51	0.80	1.21	0.58
3	14.10	0.45	0.37	0.41	0.56	0.98	0.54
4	13.90	0.39	0.36	0.41	0.46	0.74	0.45
5	13.40	0.34	0.34	0.36	0.45	0.68	0.44
6	12.70	0.14	0.17	0.16	0.19	0.32	0.25
7	12.00	0.11	0.11	0.09	0.13	0.20	0.16
8	11.00	0.11	0.14	0.12	0.09	0.13	0.16
9	9.70	0.14	0.13	0.10	0.11	0.16	0.33
10	7.40	0.099	0.09	0.07	0.08	0.08	0.16
11	7.00	0.059	0.06	0.04	0.05	0.07	0.12
12	6.50	0.11	0.11	0.07	0.09	0.11	0.15
13	4.57	0.0062	0.006	0.007	0.008	0.012	0.013
14	4.52	0.0062	0.007	0.005	0.007	0.010	0.013
15	4.45	0.0066	0.006	0.005	0.006	0.009	0.013
16	4.13	0.0024	0.003	0.003	0.003	0.004	0.008
17	3.98	0.0022	0.003	0.002	0.003	0.004	0.008
18	3.70	0.00094	0.001	0.001	0.001	0.002	0.004

4.4   Imager Detector-to-Detector Striping

Striping is estimated by comparing the mean values for each detector averaged over a large (480 x 640) image area. The analysis was performed on 15-minute imagery over a 6-h period from 26 November 2001 [Julian day 330] 0915 UTC through 1515 UTC. The values given in Table 4.6 are the differences between the average values for each detector from the overall image average (which is the mean or halfway between the two detector averages). Therefore striping between the two detectors of the infrared bands of the Imager is actually twice the values listed. Equivalent values for GOES-11 are given for comparison.

Table 4.6: GOES-12 Imager Striping Compared to GOES-11.

Imager Band	Central Wavelength (μm)	GOES-12	GOES-11
		(GVAR count, 10-bit, 0-1023)	
2	3.9	0.35	0.25
3	6.5 / 6.7	0.30	One detector only
4	10.7	1.0	0.55
5	12.0	No band	1.5
6	13.3	One detector only	No band

4.5   Imager-to-Imager Comparison

At 1805 UTC on 5 November 2001 [Julian day 309] GOES-12 was switched to one that matched the schedule of GOES-10. A comparison between the GOES-10 and GOES-12 Imagers revealed good agreement in brightness temperatures at the mid-point between the two satellites (0ºN, 112.5ºW) as shown in Table 4.7. The band-3 difference of 2.3 K was due to the differing spectral response functions. The brightness temperatures differences closely agree when this is taken into account. (See: http://cimss.ssec.wisc.edu/goes/g12_report/images/G12vsG10_img.gif)

Table 4.7: Imager-to-Imager Comparison Between GOES-12 and GOES-10.

Satellite	Imager Band	Radiance (mW/(m²·sr·cm⁻¹))	Temperature (K)
GOES-10	2 (3.9 μm)	0.628	289.8
GOES-12		0.598	289.6
GOES-10	3 (6.7 μm)	9.061	255.2
GOES-12	3 (6.5 μm)	8.486	257.5
GOES-10	4 (10.7 μm)	92.556	288.5
GOES-12		92.917	288.4

4.6   Imager-to-Polar-Orbiter Comparisons

NOAA-15 HIRS and AVHRR data were collected during the checkout period near the GOES-12 sub-satellite point. Infrared (IR) window data (HIRS, AVHRR, and GOES-12) and water vapor (WV) band data (HIRS and GOES-12) were collected within 30 min of polar-orbiter overpass time. During the checkout period there were 21 comparisons for NOAA-15 in the IR window, and 22 comparisons for the WV. The results are presented in Table 4.8. The mean brightness temperature difference for these comparisons showed GOES-12 colder than NOAA-15 HIRS by approximately 0.3 K in the IR window. GOES-12 was slightly colder than NOAA-15 AVHRR in the IR window (by less than 0.1 K). In the WV band GOES-12 was colder than NOAA-15 HIRS by 0.1 K. These results for these comparisons with GOES-12 are similar to the results of the most recent comparisons of GOES-8 and GOES-10 to polar-orbiter data, with the exception

of the WV band comparison between GOES-12 and NOAA-15 HIRS. This is likely due to the difference between the new GOES-12 WV band and the old GOES WV bands, though this bears further study and should be observed closely when GOES-12 becomes operational.

Table 4.8: Comparison of GOES-12 to NOAA-15 AVHRR and HIRS for the IR window and water vapor (WV) bands.

Comparison (satellites and band)	Mean of Absolute Differences (K)	Mean Difference (K)	Standard Deviation of Differences (K)
GOES-12 minus NOAA-15 HIRS IR window	0.64	-0.29	0.72
GOES-12 minus NOAA-15 AVHRR IR window	0.14	0.	0.18
GOES-12 minus NOAA-15 HIRS water vapor (WV)	0.77	-0.12	1.08

4.7   Calibration

4.7.1   Bias Mode (Sounder)

There was a change to the GOES-12 Sounder calibration bias mode (from Mode 1 to Mode 2) on 11 October 2001. Prior to the change there was banding evident in bands 12 and 15. (Banding occurs for groups of lines between the 2-minute calibrations of the Sounder, as opposed to line-to-line striping between the four different Sounder detectors.) The banding was most evident at approximately 0400 UTC. Infrared calibration bias factors may vary as the temperatures of instrument optical components vary. Between space looks, this variation may appear as banding in the imagery. Switching to Mode 2 reduced banding in band-12 and band-15. This updating is most important during certain parts of the day when optics temperatures are changing rapidly. Calibration bias mode 2 allows the bias factors (intercepts) to be calculated more frequently (between space looks) and is estimated based on its correlation with the variation in optics temperature. Sounder space looks occur every 2 min. A comparison for band-12 at 0346 UTC on 11, 12, and 13 October reveals reduced striping after switching to Mode 2. The switch to bias mode 2 occurred on 11 October but the elimination of banding did not take place until 13 October (see Figure 4.7). This is due to the fact that the optics temperature used for regression in Sounder calibration was not updated until 12 October.
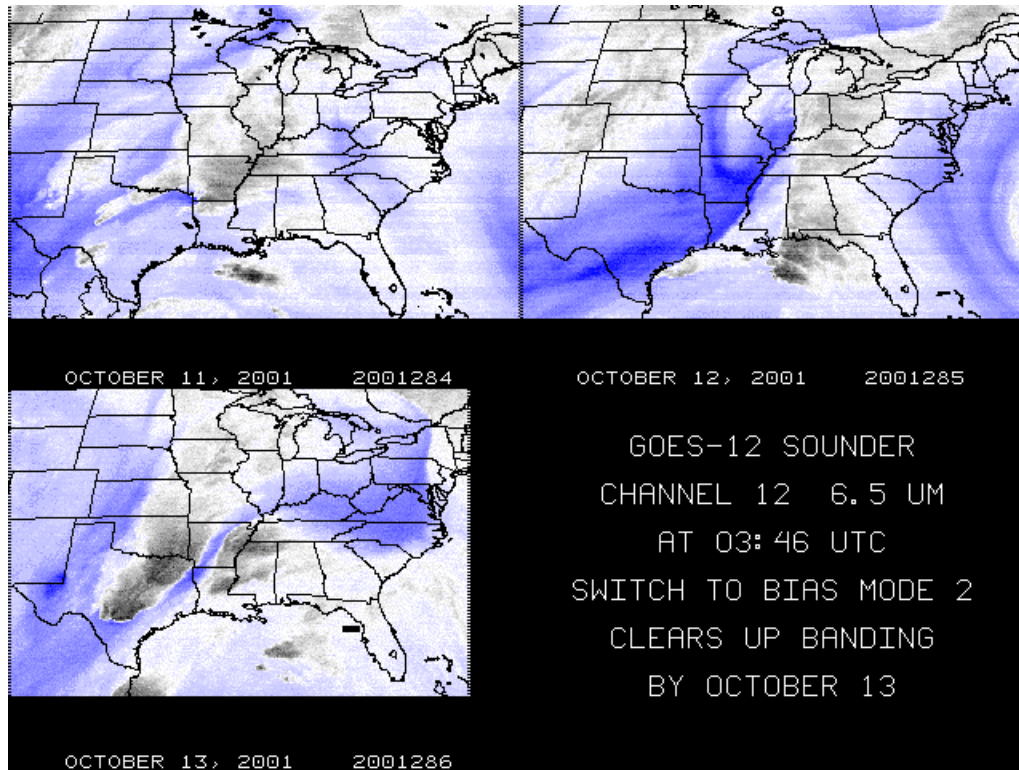
22

Figure 4.7: GOES-12 Sounder band-12 both before and after the bias mode change. Note there is less "banding" by 13 October 2001.

4.7.2 *Scan-Mirror Emissivity Coefficients (Sounder and Imager)*

On 11 October 2001 SOCC installed a new set of scan-mirror emissivity coefficients (Weinreb et al. 1997) in the GOES-12 calibration for both the Imager and the Sounder. These coefficients are used in the algorithm that corrects for the east-west scan-angle dependence of the emissivity (and reflectance) of the Imager and Sounder scan mirrors. Earlier, the GOES-12 calibration had used emissivity coefficients calculated from a previous GOES. The new coefficients were specific to GOES-12, as they were derived from on-orbit GOES-12 data. A before and after plot shows how the change was verified by comparing space-looks on the west and east side of two images. The "before" (red) line is from 11 October 2001 at 1415 UTC (see Figure 4.8). The "after" (blue) line is from 11 October 2001 at 1445 UTC. Note that the y-axis (radiance) of the plot has been limited to show the space-view. In the middle of the x-axis the earth-view pixels are scaled off the y-axis of the plot. There is definite improvement in the after image. The change is most evident in Imager band-6.
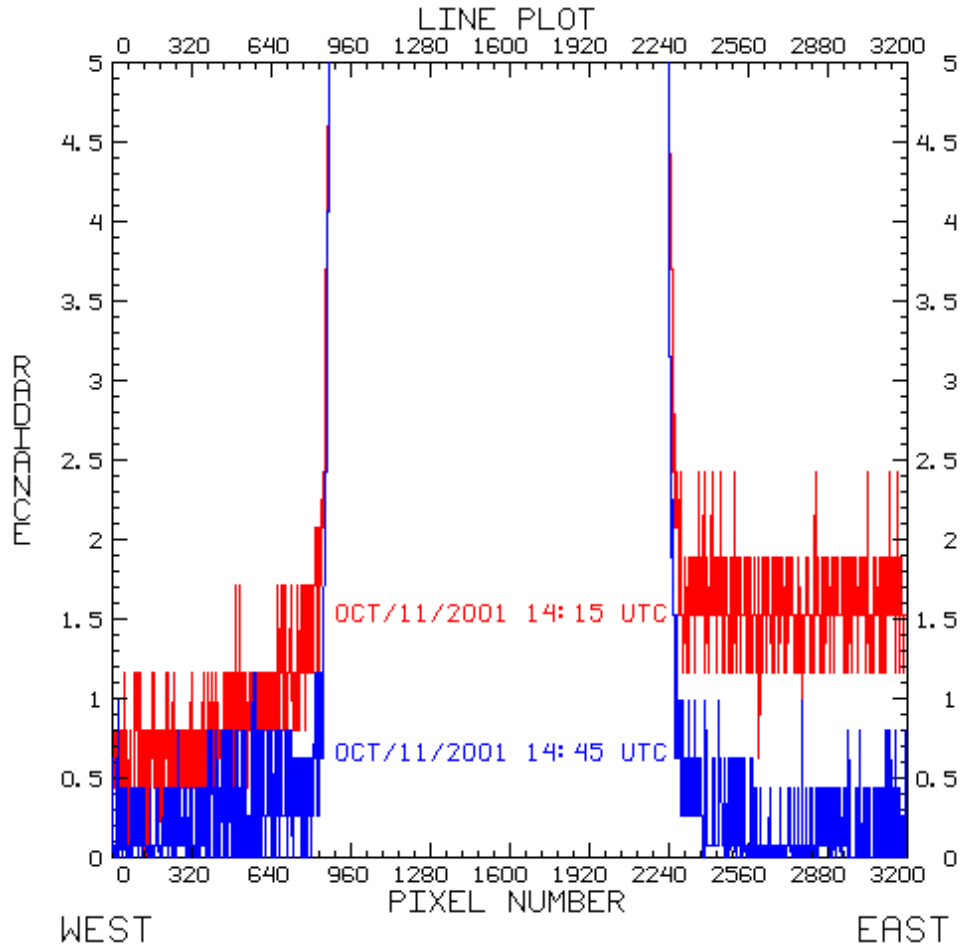
Figure 4.8: Comparison of space-looks on the west and east sides of two images, before (red line) and after correction (blue line), showing the closer agreement between the space views after installing a new set of scan-mirror emissivity coefficients.

4.7.3 Imager-to-Imager Comparison

The Imager-to-Imager comparison is based on GOES-08/10/12 Imager data collected every half hour from 2345 UTC on 11 November 2001 to 2315 UTC on 16 November 2001. This time period is chosen for its most complete overall data coverage for five consecutive days. The spatial coverage of the images extends from 0ºN to 40ºN to include both land and sea. Accordingly, analyses were usually done for land, sea, and all pixels. During this period of time GOES-8/10/12 were located at 75ºW, 135ºW, and 90ºW, respectively. To minimize the differences due to view angles, the data were limited to between 81ºW and 84ºW for the GOES-8/12 comparison and between 111ºW and 114ºW for the GOES-10/12 comparison.

4.7.3.1 Visible Band

Measurements in the visible bands of different spacecraft are not expected to be identical since these bands lack on-board calibration. It is thus useful to know how much the operational satellites have degraded, using the new satellite as reference. Figure 4.9(a) is a scatter plot of

albedo from the two operational satellites as a function of GOES-12 albedo. While the GOES-8 albedo measurements are consistently smaller than those of GOES-12, it was initially puzzling why some GOES-10 albedo measurements are comparable to those of GOES-12 and some are much smaller. It was later realized that this was the result of the combination of solar angle and topography. When the sun is east of 90ºW, GOES-12 views the illuminated side of mountains whereas GOES-10 views the dark side. Thus GOES-10 albedo measurements are much smaller than those of GOES-12. When the sun is west of 135ºW, the opposite is true, as indicated by the different color of "+" in Figure 4.9(a). Indeed, such scatter is more pronounced for land targets (not shown). The GOES-8 data did not show such scatter because the two satellites are much closer to each other and, secondarily, the land is relatively flat in the region of comparison.
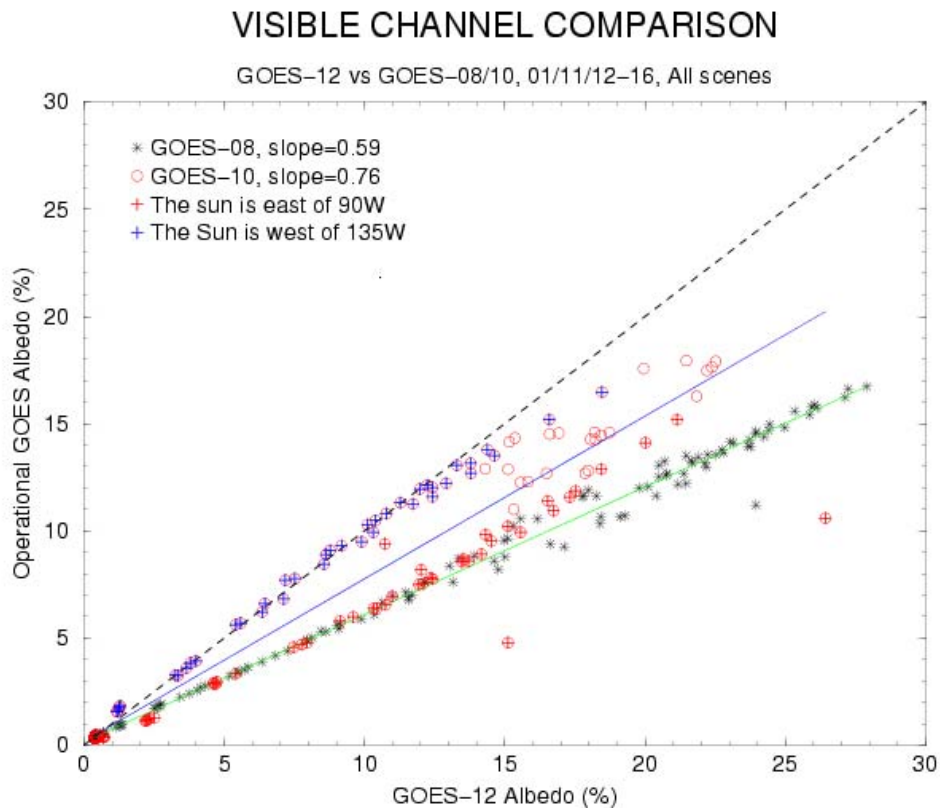

Figure 4.9(a): Scatter plot of GOES-8 (*) and GOES-10 (°) reflectance as a function of GOES-12 reflectance. For GOES-10, the morning (red +) and afternoon (blue +) samples are further separated. Reflectance is the arithmetic mean of pixel reflectance within the area of comparison. The dashed line at a 45-degree angle is shown for reference. The thin solid lines are least-squares regression lines, where the slopes indicate the sensitivity of the operational GOES relative to GOES-12.

To eliminate this scatter, the data is further restricted to the local noon of target. Each of five targets of 40° in north-south dimension is divided into 20 segments of 2° each to increase the number of samples. The results are shown in Figure 4.9(b). Compared to Figure 4.9(a), the

scatter for GOES-10 is much removed, but the slopes for both GOES-8 and 10 are remarkably robust. In fact, this is also true for land-only and sea-only targets (not shown).

VISIBLE CHANNEL COMPARISON
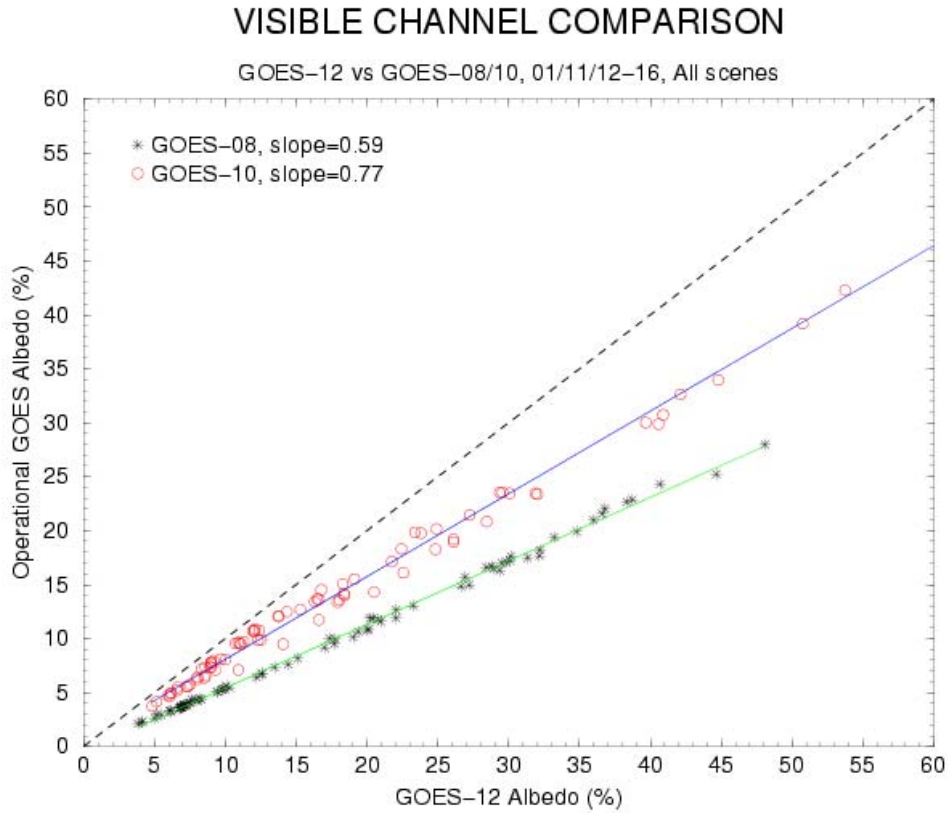
GOES−12 vs GOES−08/10, 01/11/12−16, All scenes

Figure 4.9(b): Similar to Figure 4.9(a), but limited to local noon cases only. See text for details.

From Figure 4.9(b), in November 2001, the visible band sensitivity of GOES-8 (10) was about 59% (77%) that of GOES-12, and the sensitivity of GOES-8 was about 0.59/0.77 = 77% that of GOES-10. To gain more perspective, these results are plotted in Figure 4.9(c), together with results from previous intercomparison exercises. If the Spectral Response Function (SRF) of visible bands of all these satellites were identical, the sensitivities were perfect before launch, dropped to a constant shortly after launch, and then degraded exponentially, the symbols in Figure 4.9(c) should form an exponential curve. In reality, the SRF are different (except that GOES-10 and GOES-12 are almost identical), which can result in different measurements over vegetation. Some of these ambiguities can be greatly reduced if the samples are limited to ocean only and a radiative transfer model is used to characterize the SRF difference. Figure 4.9(d) shows the Imager visible SRF for GOES-8/12. Note that both GOES-11 and GOES-12 extend past the vegetation transition zone near 0.72 μm.
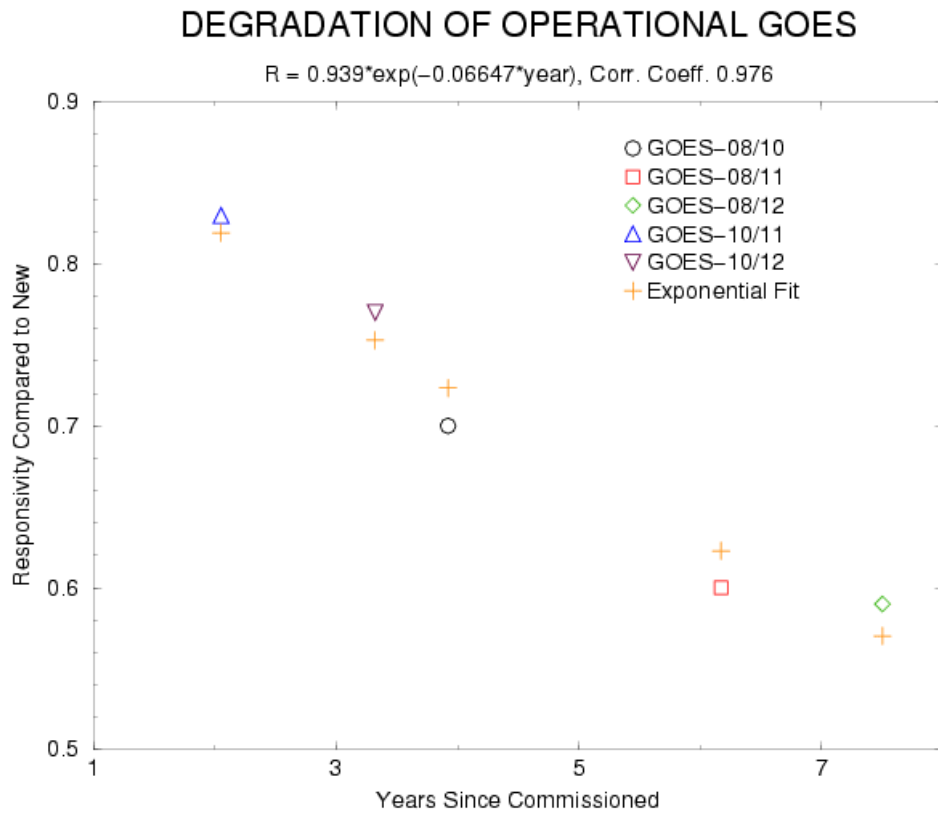
Figure 4.9(c): Visible band sensitivity of operational satellites relative to a recently commissioned satellite.
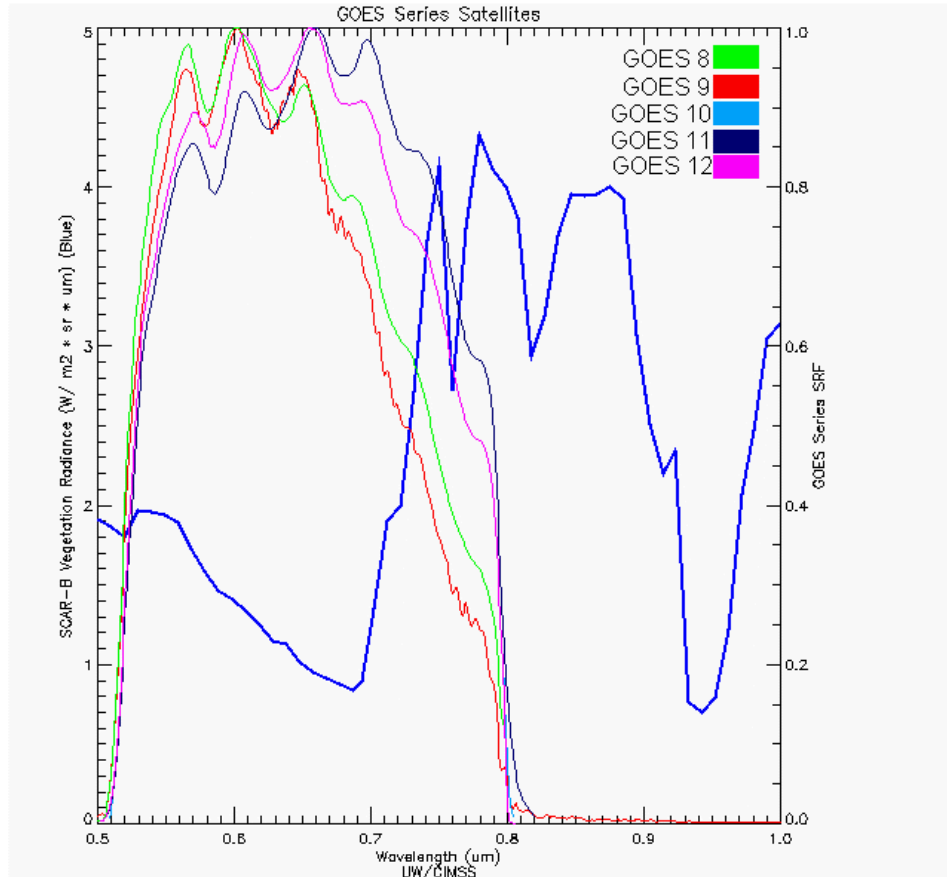
Figure 4.9(d): GOES Imagers (8/9/10/11/12) visible band spectral response functions. An AVIRIS (Airborne Visible InfraRed Imaging Spectrometer) spectra (dark blue line) is also shown to demonstrate the transition zone near 0.72 μm.

4.7.3.2 Infrared Bands

The infrared bands should be well calibrated without systematic bias among the Imagers, except that the spectral response function of the water vapor band (6.5 μm) on GOES-12 was designed to be quite different from those on GOES-8/11, which can cause large difference in brightness temperature. This spectral widening was needed to acquire more signal from the smaller FOV (Schmit et al. 2001). Table 4.9 shows the mean brightness temperature differences between the GOES-12 Imager and the GOES-8/10 Imagers for bands 2-4. As expected, the brightness temperature differences between GOES-12 and GOES-8/10 for the 3.9 and 11 μm bands are small (less than 0.25 K), whereas the difference for the 6.5 / 6.7 μm band is about 3 K. Over 2 K of this is due to the SRF differences alone.

Table 4.9: Mean brightness temperature difference (K) between the GOES-12 Imager and the GOES-8 and 10 Imagers for the IR bands.

Imager band	Ocean		Land		Ocean and Land	
	G12-G08	G12-G10	G12-G08	G12-G10	G12-G08	G12-G10
3.9 μm	-0.23	-0.21	-0.14	-0.07	-0.20	-0.10
6.5 / 6.7 μm	+2.54	+2.96	+3.01	+2.98	+2.70	+2.98
11 μm	-0.09	+0.13	-0.04	+0.21	-0.07	+0.19

Time series of the brightness temperature differences are plotted in Figure 4.10 to examine the consistency of the overall agreement or difference between GOES-12 and GOES-8 and GOES-10. In Figure 4.10(a & b), a distinctive pattern of daily variation is apparent for the 3.9 μm band, especially for the GOES-12/10 comparison and, to a lesser degree, for the 11 μm band of the GOES-12/10 comparison. This can be explained by the same mechanism that causes the daily variation of GOES-12/10 visible band difference [Figure 4.9(a)]. Inspection of the time series (Figure 4.10(a)) indicates that the GOES-12 and GOES-8 brightness temperature difference is small and stable for the 11 and the 3.9 μm bands (at night). The difference for the 6.5 / 6.7 μm band is large (due to the differing SRF) but stable. For GOES-12 and GOES-10, no such conclusion can be convincingly drawn, largely because the two satellites were located sufficiently far apart that they viewed the same earth target through significantly different atmospheres and with different insolation conditions.
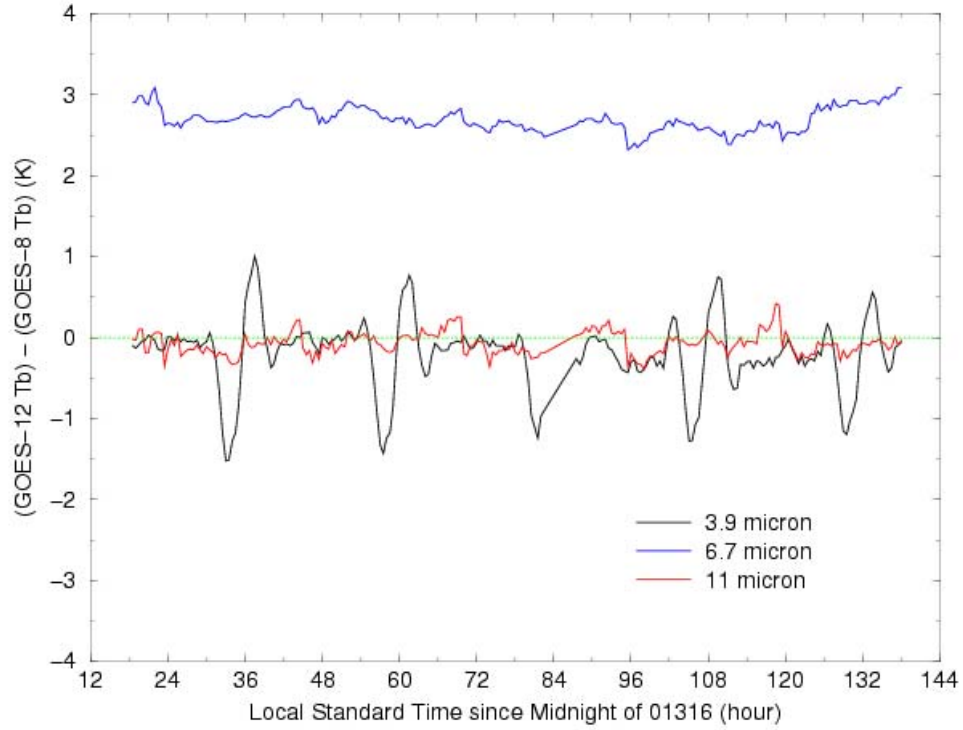
Figure 4.10(a): Brightness temperature difference [(GOES-12) – (GOES-8)] during the period of comparison. The brightness temperatures are arithmetic means of individual pixel values within the area of comparison.
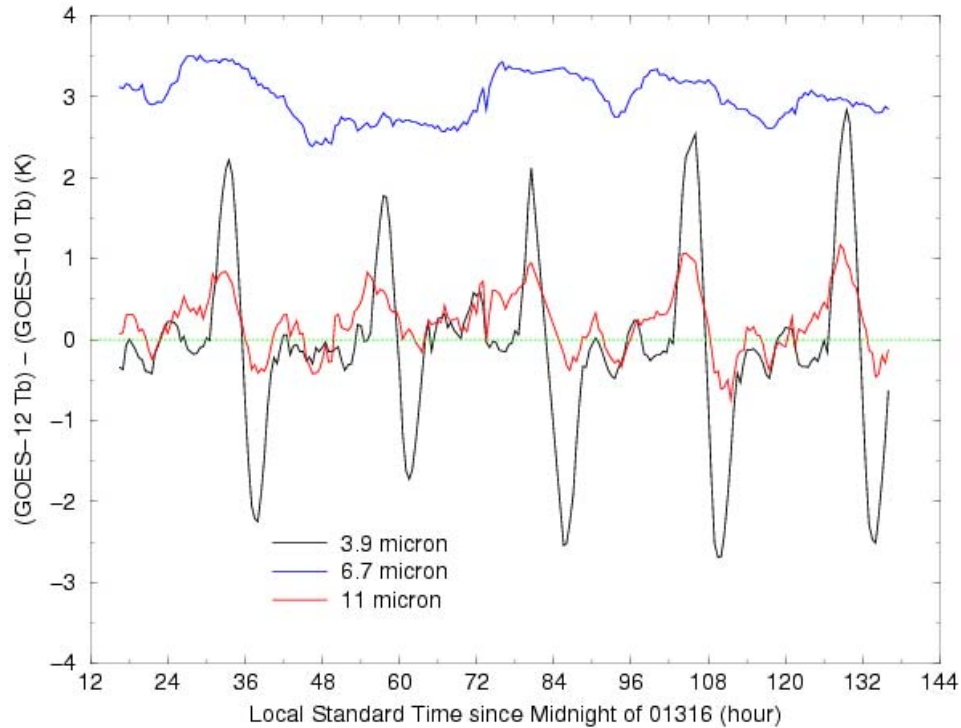
Figure 4.10(b): Same as Figure 4.10(a), but for GOES-12 – GOES-10.

To further refine the comparisons, Figure 4.10(a & b) are duplicated for ocean scenes only (Figure 4.10(c & d)). Little difference is observed between the GOES-12/8 comparisons (Figure 4.10(a & c)). For GOES-12/10, there is little change in the 6.5 / 6.7 µm band, because that band has little dependence on the earth's surface. However, the daily variation in the 3.9 µm band differences is noticeably reduced and that for the 11 µm band almost disappears. Even so, the GOES-12/10 ocean-only daily-variation (including the 3.9 µm band at night), though not as periodic as the variations in Figure 4.10(b), are still larger in amplitude than the variations seen for GOES-12/8 (Figure 4.10(a & c)).

Another feature (or the lack thereof) confirmed by Figure 4.10(c & d) is that, unlike GOES-11, there is no unexplained variation at local midnight for GOES-12.
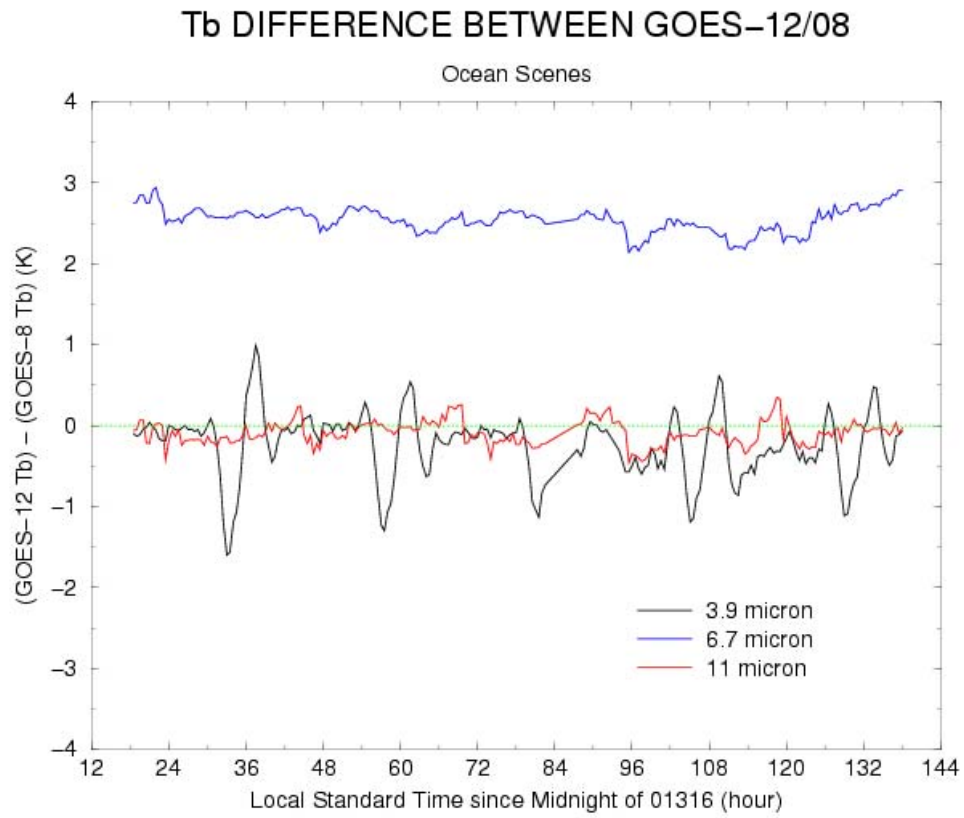
Figure 4.10(c): Same as Figure 4.10(a), but over ocean only.
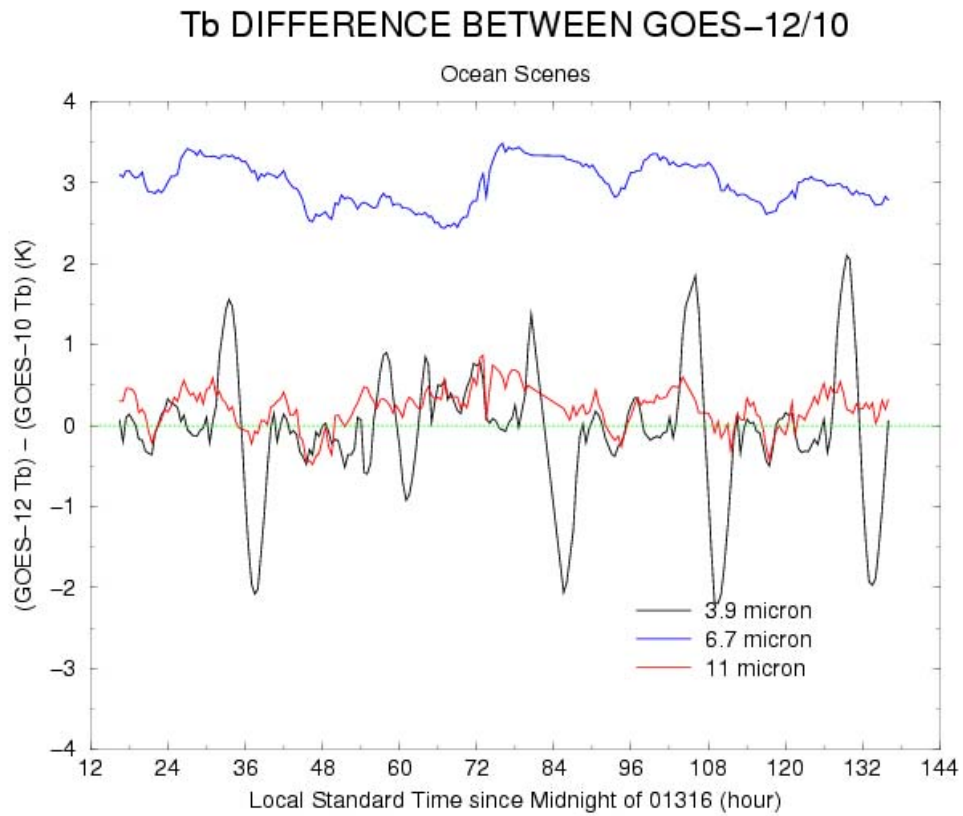
Figure 4.10(d): Same as Figure 4.10(b), but over ocean only.

Histograms of the brightness temperature differences are presented in Figures 4.11(a) and 4.11(b). They show no dependence of the differences on scene temperature.

Figure 4.11(a): Histograms of GOES-12/08 brightness temperatures over the region of comparison for one night. The agreement for the 3.9 and 11 μm bands, as well as the difference for the 6.5 / 6.7 μm bands, are persistent for all T_b measurements.
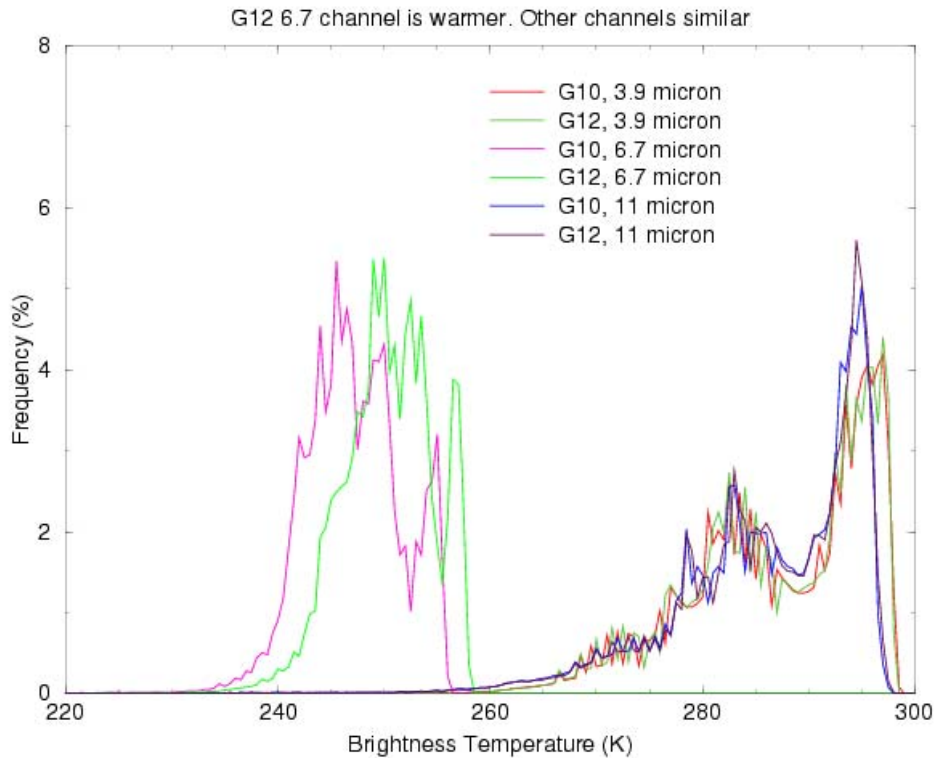
Figure 4.11(b): Same as Figure 4.11(a), but for GOES-12/10.

4.7.4 Imager-to-Sounder Comparison

Between 11 and 16 November 2001, when the Imager-to-Imager comparison was made, the GOES-12 Imager was also synchronized with Sounder, making the Imager-to-Sounder comparison m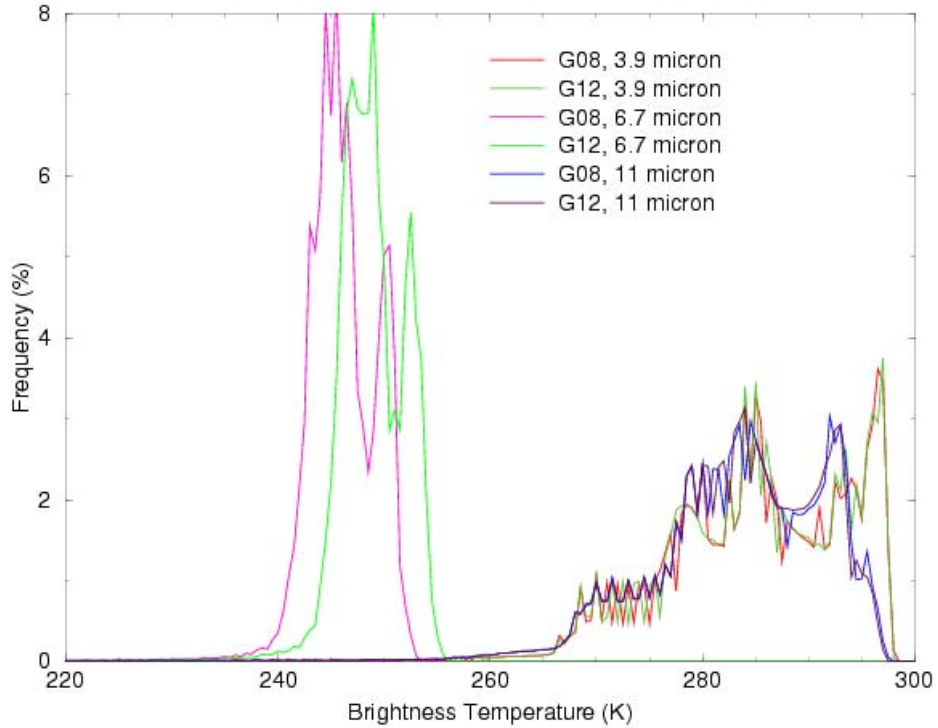ore valid. In this comparison, the results of which are reported in Table 4.10, Imager band-1 is compared with Sounder band-19; Imager band-4 is compared with Sounder band 8; Imager band-6 is compared with Sounder band-5; Imager band-2 is compared with the mean of Sounder bands 17 and 18; and Imager band-3 is compared with the mean of Sounder bands 11 and 12. In addition, the time series of these differences are plotted in Figure 4.12.

Table 4.10: Mean difference between the GOES-12 Imager and Sounder. No correction for the different spectral response functions was applied.

Visible	3.9 µm	6.5 / 6.7 µm	11 µm	13.3 µm
+0.38%	-1.10 K	+3.72 K	-0.05 K	+2.00 K

The overall differences for the first three bands could be due to spectral response differences, and the differences for the last two bands are reasonably small. It is interesting, however, that the Imager-Sounder differences are quite similar to the Imager-Imager differences, which could result from a less-well-calibrated GOES-12 Imager compared with a well-calibrated GOES-12 Sounder and GOES-08/10 Imagers. Figure 4.12 also depicts a rather obvious diurnal variation of the differences, particularly for the 6.5 / 6.7 and 11 μm bands. The minima occurred closer to the satellite midnight, which is one hour later than the local midnight. This is more likely caused by calibration uncertainties.
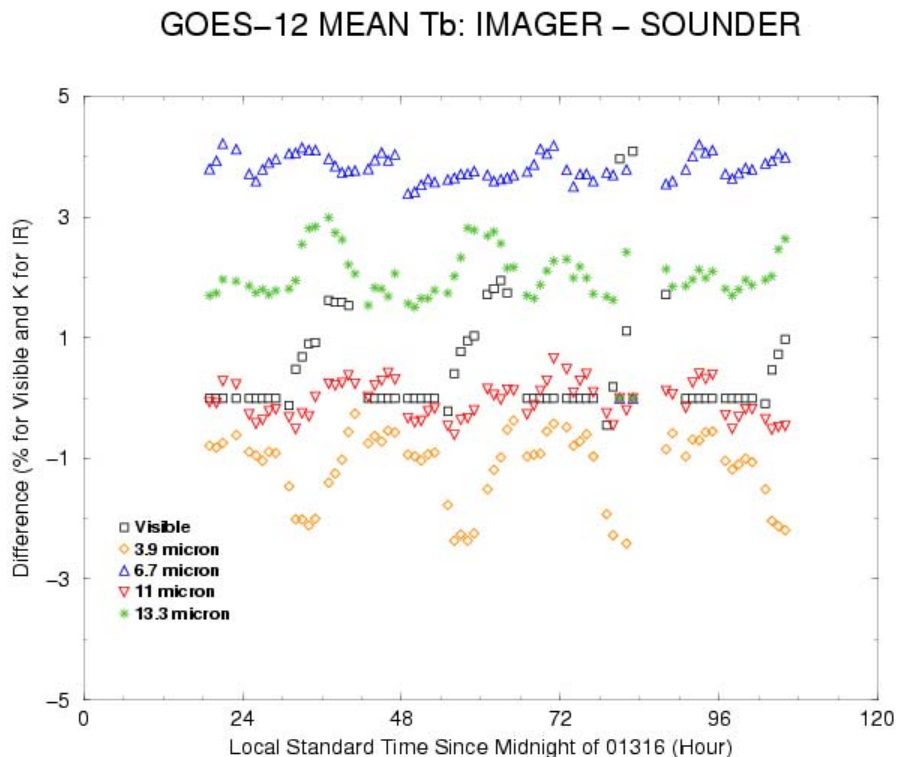

Figure 4.12: Differences of GOES-12 Imager and Sounder brightness temperatures for the IR bands (or percent albedo for the visible band) plotted as a function of time. No correction for the different spectral response functions was applied.

The difference for the 13.3 μm band is expected because, for this band, the spectral response function for the Imager is broader than that for the Sounder; therefore, the Imager is more responsive to the lower (and usually warmer) part of the atmosphere. For a typical clear-sky condition, forward radiative transfer model calculations show this difference to be approximately 1.5 K. The difference for the visible band is reasonably small although, as for GOES-11, it seems that the difference is proportional to the mean illumination (peaking at noon). The difference for the 11 μm band is small and nearly random, which probably is largely due to the difference in spatial resolution of the two sensors. Finally, the mean differences for the 3.9 and 6.5 / 6.7 μm bands are partially explained because of the band averaging for the Sounder (see Figure 4.13).
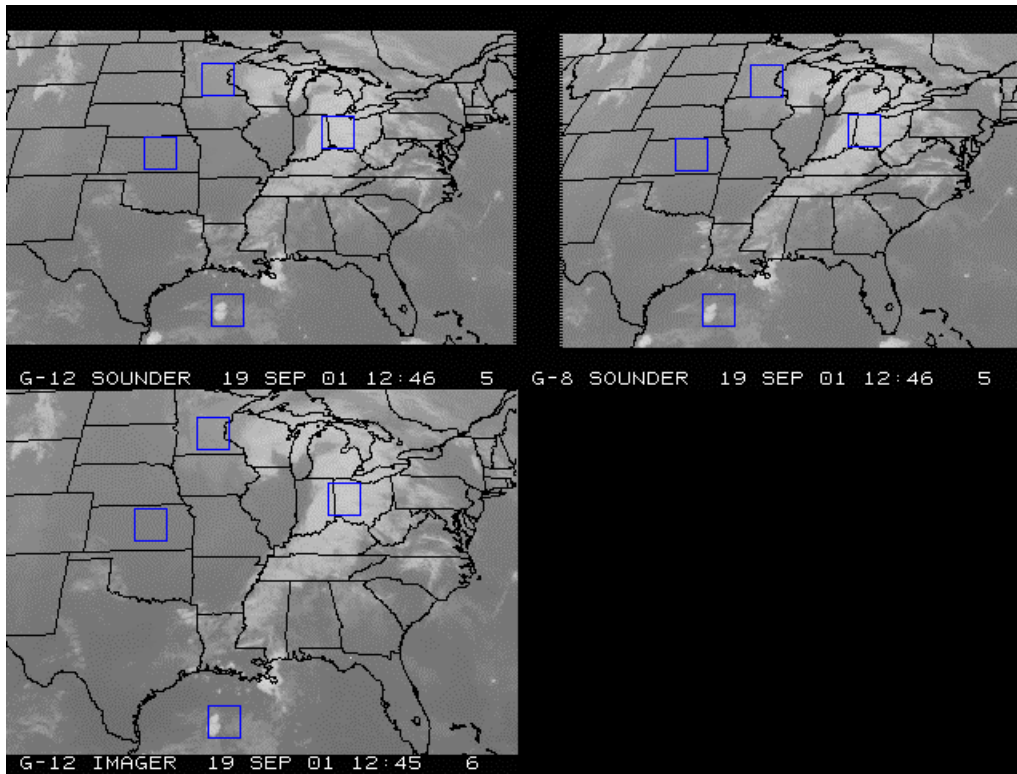
Figure 4.13: Comparison of GOES-12 Sounder and Imager to GOES-8 Sounder for the 13.3 μm band. The boxes correspond to regions noted in the tables below.

Site #1 (Ohio/Indiana)

Instrument	# Pixels	Min. Temp. (K)	Max. Temp. (K)	Ave. Temp. (K)	Stand. Dev.
GOES-12 Sounder	441	215.6	239.6	222.6	3.697
GOES-8 Sounder	441	215.0	238.7	222.4	3.681
GOES-12 Imager	3362	216.2	242.0	223.3	3.253

Site #2 (Kansas)

Instrument	# Pixels	Min. Temp. (K)	Max. Temp. (K)	Ave. Temp. (K)	Stand. Dev.
GOES-12 Sounder	441	262.7	265.8	264.1	0.595
GOES-8 Sounder	441	259.7	263.0	261.4	0.658
GOES-12 Imager	3362	265.4	267.5	266.4	0.393

Site #3 (Minnesota)

Instrument	# Pixels	Min. Temp. (K)	Max. Temp. (K)	Ave. Temp. (K)	Stand. Dev.
GOES-12 Sounder	441	247.9	257.4	253.7	1.323
GOES-8 Sounder	441	243.8	256.0	251.8	1.412
GOES-12 Imager	3362	249.3	259.7	255.0	1.240

Site #4 (Gulf of Mexico)

Instrument	# Pixels	Min. Temp. (K)	Max. Temp. (K)	Ave. Temp. (K)	Stand. Dev.
GOES-12 Sounder	441	208.8	270.3	258.2	15.135
GOES-8 Sounder	441	214.4	267.8	256.9	14.348
GOES-12 Imager	3362	215.9	271.9	258.9	16.002

Forward radiative transfer model calculations for a clear-sky standard atmosphere show the GOES-12 Imager 13.3 μm band will have a slightly higher (1.5 K) mean brightness temperature than the Sounder band-5 (Schmit et al. 2001).

4.7.5   Sounder-to-Sounder Comparison

A preliminary comparison is available in an animated format (http://cimss.ssec.wisc.edu/goes/g12_report/anis/anigsare.html), showing remapped imagery from all 19 bands from both the GOES-12 and GOES-8 Sounders at 2046 UTC on 20 September 2001. Additional time periods are also available and can be examined via the CIMSS GOES-12 Web page (http://cimss.ssec.wisc.edu/goes/realtime/g12/arc/). Favorable overlap in coverage between the satellites is considerable. Although patterns and overall ranges match reasonably well, some differences are obvious. GOES-12 Sounder data appear markedly less noisy (than GOES-8 data). GOES-12 Sounder visible data appear brighter. Some initial differences between the observed radiances from the two satellites result from known differences in the respective spectral response functions.

Another Sounder radiance comparison, from late in the GOES-12 Science Test at 1846 UTC on 20 October 2001, is presented in Figure 4.14. There is favorable overlap in the coverage between the satellites, following re-mapping of the imagery to a common (Mercator) projection. Each of the 19 different spectral bands from the GOES-12 and GOES-8 Sounders is presented in a multi-panel format. Band-1 is shown in panel 1, starting in the upper left, with subsequently numbered bands following across rows and then down columns. The domain covers only the central and eastern US as seen from GOES-12 (a map has been added to panel 1). A single color enhancement is applied to all 18 infrared bands, while the visible (band-19) is shown in shades of gray. Although patterns and overall ranges match reasonably well, some differences are obvious. GOES-12 Sounder data appear markedly less noisy than GOES-8 data. For example, note bands 1 and 15.

Diurnal (24 h) animation loops further provide the viewer with the temporal nature of the ever changing atmosphere, enhancing the spatial and spectral characteristics presented in the imagery from any individual time period (http://cimss.ssec.wisc.edu/goes/realtime/anigeall.html).
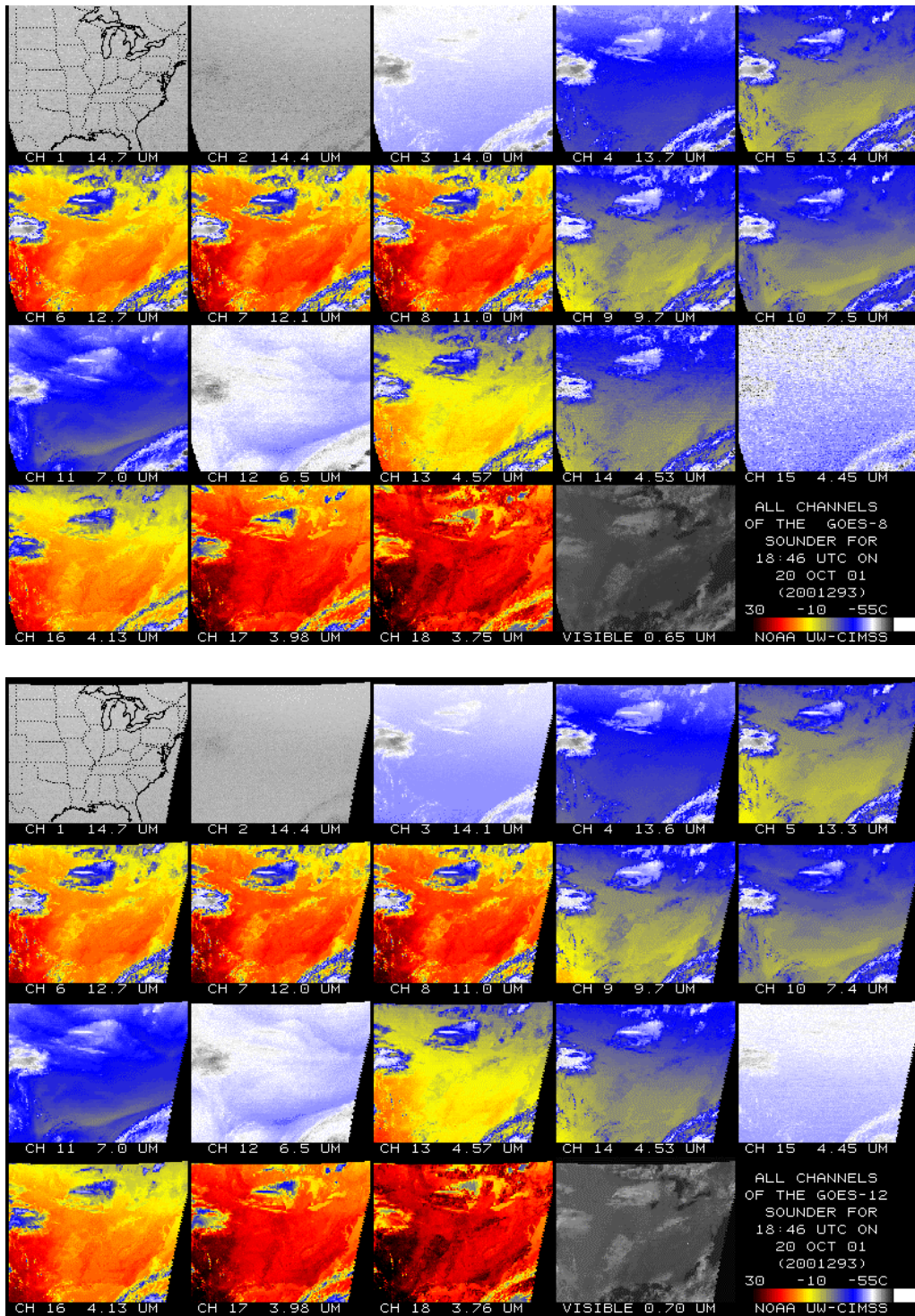
Figure 4.14: All 19 bands from both the GOES-8 (top) and GOES-12 (bottom) Sounders at 1846 UTC on 20 October 2001.

In order to quantify these differences, Sounder brightness temperature differences were computed for all 18 infrared bands from the GOES-8 and GOES-12 Sounders for a one night-time period. These differences are shown in Figure 4.15. The operational spectral response

functions were used for both GOES-8 and GOES-12 and only values of similar look angles were compared. It is evident that the GOES-12 Sounder brightness temperatures match those from GOES-8 for most bands. The GOES-12/8 comparison shows large differences (2 K and -6 K) in bands 2 and 15 that are most likely due to uncertainties in the GOES-8 spectral response functions.
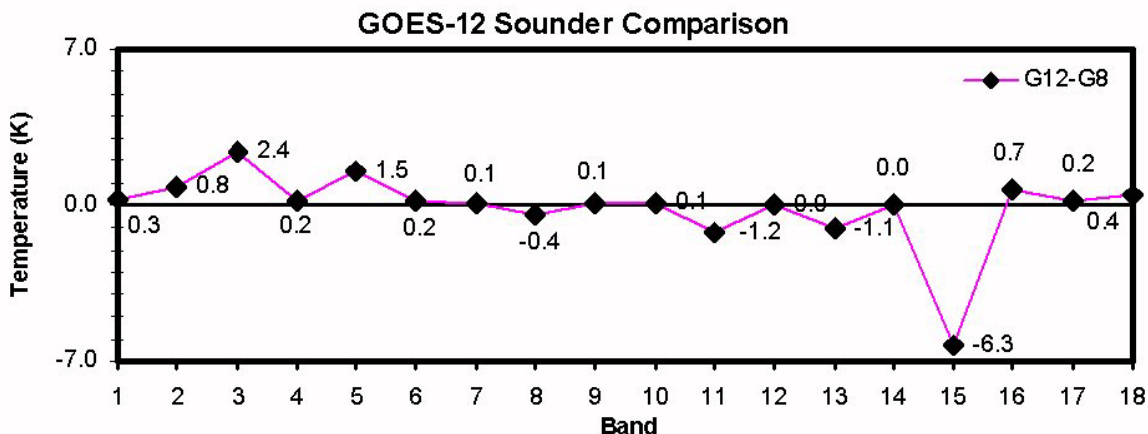

Figure 4.15: Brightness temperature differences between the GOES-12 and GOES-8 Sounders.

5.0   Product Validation

A number of products were generated with data from the GOES-12 instruments and then compared to products generated from other satellites or ground-based measurements.

5.1   Total Precipitable Water (TPW) from Sounder

Total precipitable water retrievals (displayed in the form of an image) for GOES-8 and GOES-12 are presented in Figure 5.1 over the same area at approximately the same time (1846 UTC on 20 October 2001). These retrievals are generated from clear radiances in a 3x3 FOV scene. Radiosonde measurements of TPW are plotted on top of the images. Qualitatively, there is good agreement between the GOES-8 and GOES-12 TPW retrievals that, in turn, compare reasonably well with the reported radiosonde measurements of TPW. When a comparison between two satellites is done like this, one must consider several items.
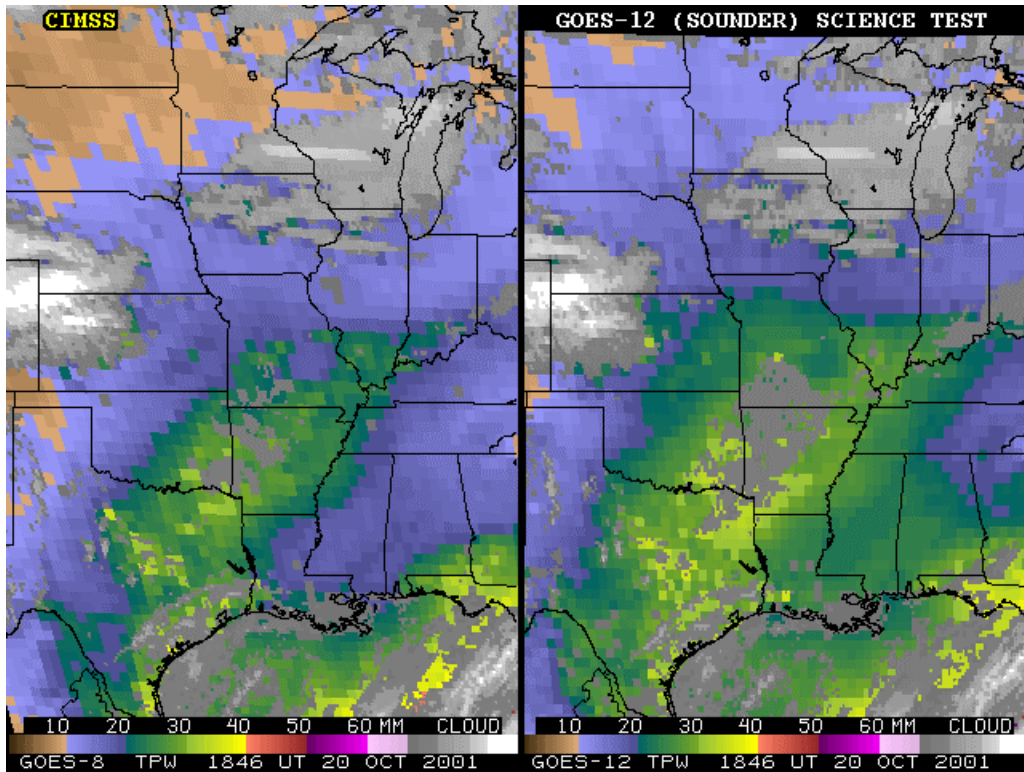
Figure 5.1: GOES-8 (left) and GOES-12 (right) retrieved total precipitable water (TPW) from the Sounder displayed as an image. The data are from 1846 UTC on 20 October 2001.

First, while the start scan line times were identical for the GOES-12 and GOES-8 Sounder images, the individual measurements are not exactly time coincident due to the differing scan sector widths. Second, due to different satellite orbital locations, even precisely co-located fields-of-view are seen through different atmospheric paths. Both of these factors will contribute to observed TPW differences between the two satellites.

For the period 28 October 2001 to 17 December 2001 (immediately following the GOES-12 Science Test) GOES-8 and GOES-12 TPW retrievals were collocated with radiosonde measurements of TPW at 0000 UTC and 1200 UTC each day. The GOES-8 and GOES-12 retrievals were required to be within 50 km and 60 min of each other and within 50 km and 60 min of nearby radiosonde observations. Statistics were then generated which compared the retrieved TPW and its first guess (i.e., Eta model forecast) to the radiosonde TPW. These statistics are shown in Table 5.1. Note that these retrievals were computed using radiance bias correction coefficients from GOES-10 (as default). Note: 1) All retrievals are 3x3 FOV retrievals; 2) There are at least 4 clear FOVs per retrieval; 3) All statistics contained 3229 comparisons.

Table 5.1: GOES-8 and GOES-12 Retrieval/RAOB Co-location Statistics.

Statistic	GOES-8	GOES-12	Guess	Radiosonde
TPW				
SD (mm)	1.93	1.75	1.89	
Bias (mm)	-1.00	-0.71	-0.98	
Mean (mm)	9.70	9.97	9.72	10.70
WV1 (surface to 900 hPa)				
SD (mm)	0.81	0.82	0.82	
Bias (mm)	-0.49	-0.45	-0.57	
Mean (mm)	3.42	3.45	3.34	3.91
WV2 (900 hPa to 700 hPa)				
SD (mm)	1.27	1.20	1.21	
Bias (mm)	-0.43	-0.20	-0.33	
Mean (mm)	4.30	4.52	4.39	4.73
WV3 (700 hPa to 300 hPa)				
SD (mm)	0.86	0.81	0.89	
Bias (mm)	-0.09	-0.06	-0.08	
Mean (mm)	1.93	1.96	1.94	2.02

Overall, the GOES-12 Sounder water vapor retrievals are more similar to radiosondes than those from GOES-8. The lower noise of the GOES-12 Sounder radiances likely played a role in the improved retrieval quality.

Hourly GOES-12 retrieved TPW values were also collocated in time and space with ground-based measurements of TPW by a microwave radiometer at the Cloud and Radiation Testbed (CART) site in Lamont OK for later analysis.

5.2 Lifted Index (LI) from Sounder

The lifted index (LI) product is generated from the retrieved temperature and water vapor profiles (Ma et al. 1999) that are generated from clear radiances in a 3x3 FOV scene. Figure 5.2 shows lifted index retrievals (displayed in the form of an image) for GOES-8 and GOES-12 over the same area at approximately the same time, showing some bias in the LI values.
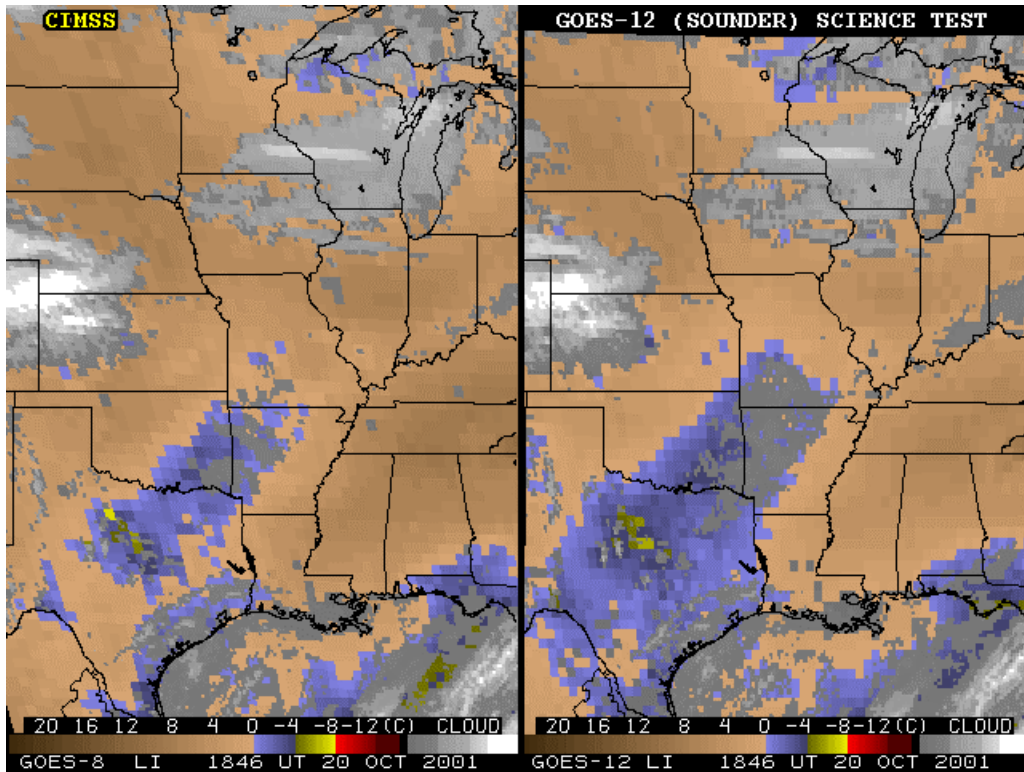
Figure 5.2: GOES-8 (left) and GOES-12 (right) retrieved Lifted Index (LI) from the Sounder displayed as an image. The data are from 1846 UTC on 20 October 2001.

5.3   Cloud Parameters

The addition of the 13 μm band on the GOES-12 Imager makes near full-disk cloud products possible. GOES-12 will provide more accurate calculations of Effective Cloud Amount (ECA) than currently available from the GOES-8 through GOES-11 Imagers, and more frequent and timely Satellite Cloud Products (SCP) in support of the Automated Surface Observing System (ASOS), in addition to the near full-disk coverage.

Figure 5.3 shows a comparison of GOES-8 and GOES-12 Sounder cloud-top pressure derived product images from 20 October 2001 at 1846 UTC. Another comparison produced just prior to the GOES-12 Science Test showed good agreement between the GOES-12 Imager and Sounder cloud-top pressure products (see Figures 5.4 and 5.5). The comparison displayed generally good correlation between the Imager-based product and that produced from the full complement of GOES Sounder bands.
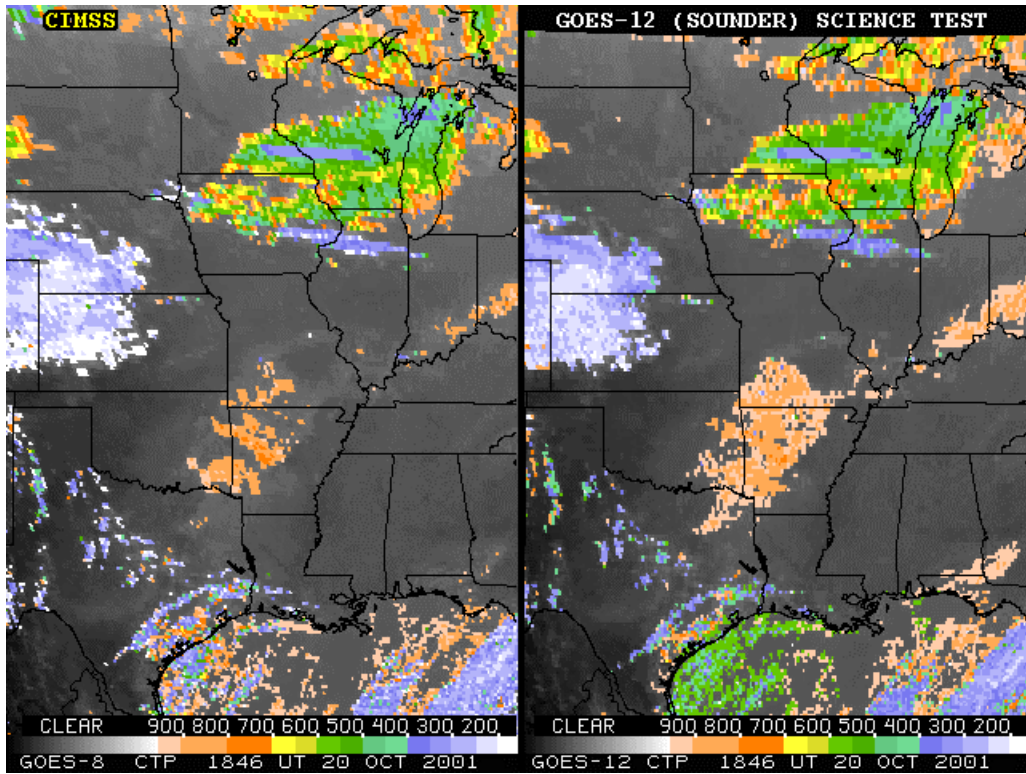
Figure 5.3: GOES-8 (left) and GOES-12 (right) retrieved cloud-top pressure from the Sounder displayed as an image. The data are from 1846 UTC on 20 October 2001.
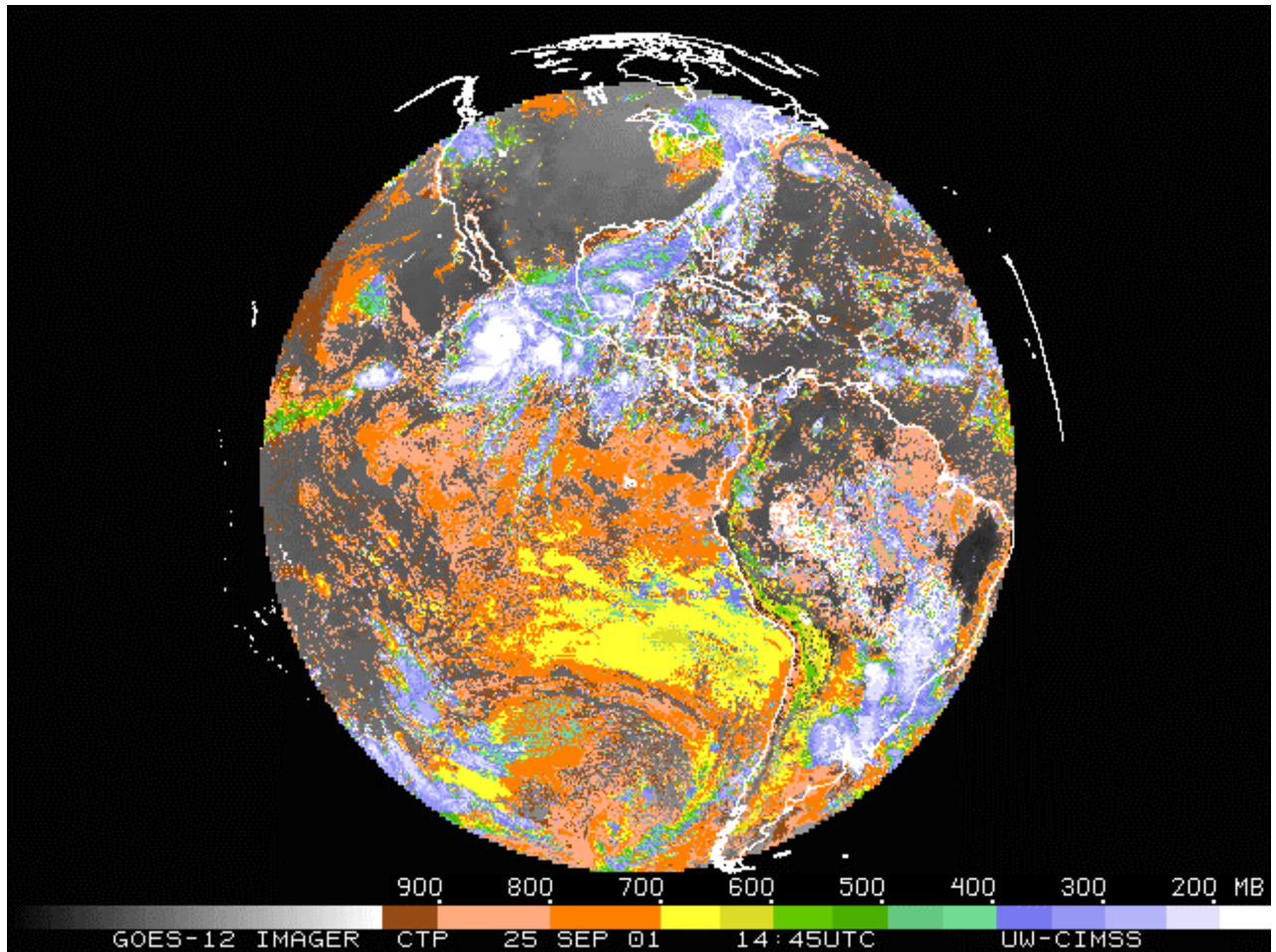
Figure 5.4: GOES-12 cloud-top pressure from the Imager from 1445 UTC on 25 September 2001.
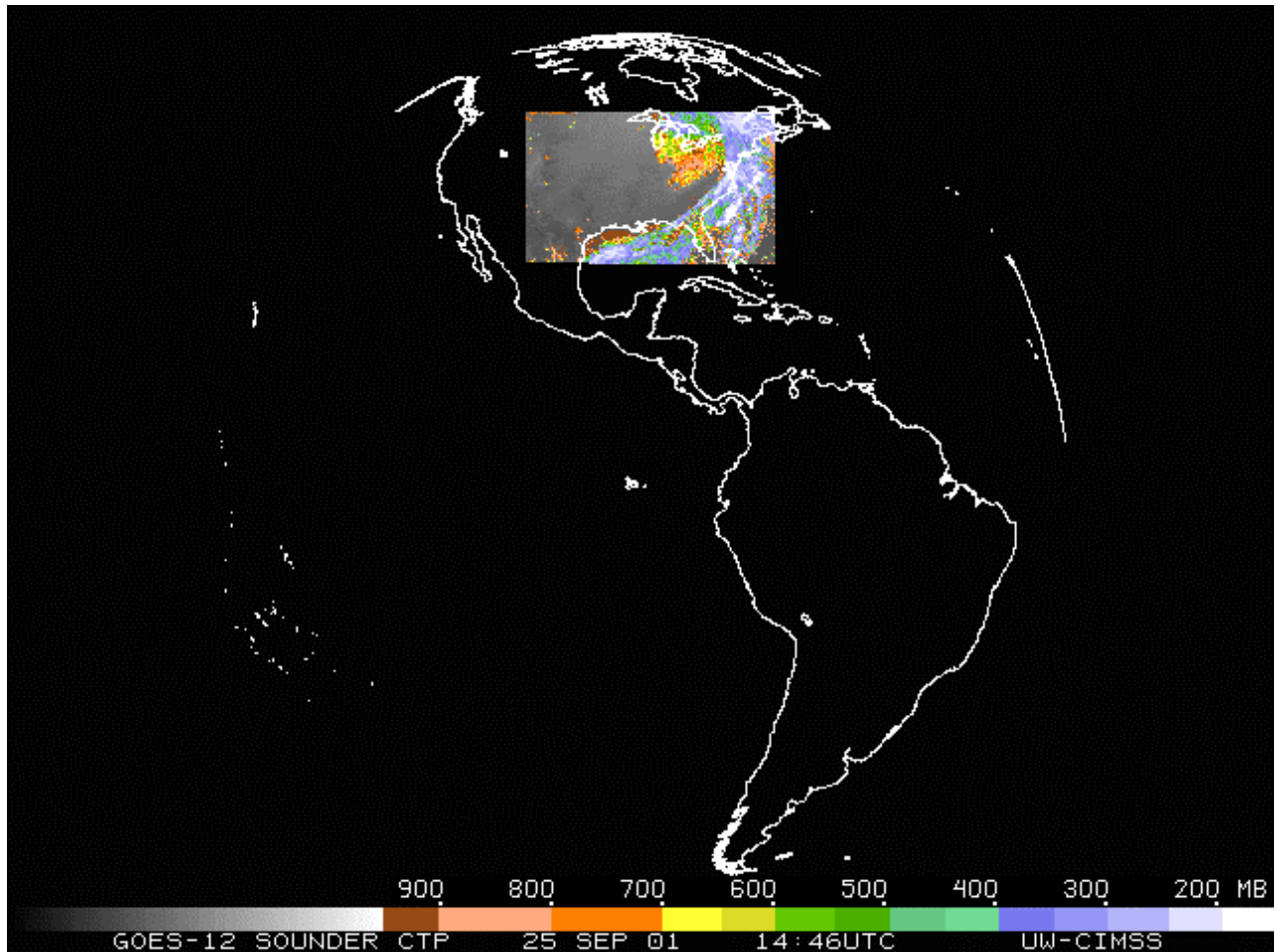
Figure 5.5: GOES-12 cloud-top pressure from the Sounder from 1446 UTC on 25 September 2001.

5.4   Satellite Winds

The changes made to the GOES-12 imager offer potential benefits to the derivation of cloud-drift and water vapor motion winds. First, the addition of the 13.3 μm band will allow, for the first time since GOES-7, the use of the well-known CO_2 slicing algorithm to assign heights to viable cloud tracers. The resultant CO_2 slicing algorithm (Menzel et al. 1983) height assignments will supplement the height assignments provided by the H_2O intercept algorithm (Schmetz et al. 1992). Second, the improved resolution of the water vapor band is expected to aid and improve the water vapor motion wind product through improved tracking of water vapor features.

The GOES high-density winds software has been significantly modified to prepare it for the GOES-12 imager instrument changes and for the adoption and use of a new radiative transfer model. The RTTOVS radiative transfer model, which has been used since the launch of GOES-8, was successfully replaced with the Pressure-Layer Optical Depth (PLOD) radiative transfer model. Wind verification statistics, for high-level tracers whose primary height assignment method is the H_2O intercept method, indicate no significant differences in wind quality when switching from the RTTOVS to PLOD radiative transfer model.

46

GOES high density winds were generated routinely for the entire GOES-12 Science Test period, and continued until 16 December 2001. Figures 5.6 and 5.7 show water vapor winds for GOES-8 and GOES-12, respectively.
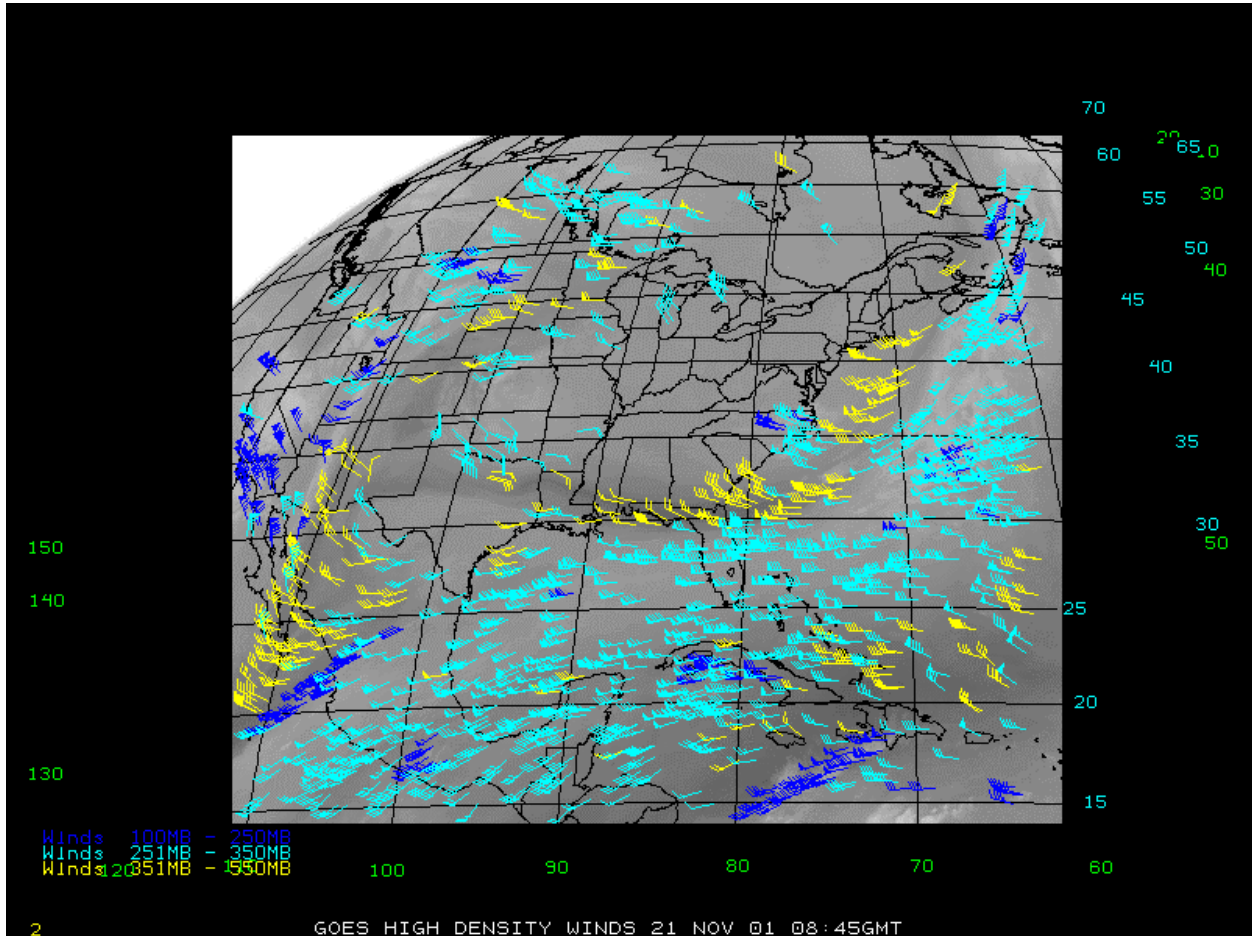

Figure 5.6: GOES-8 high-density water vapor winds. In addition to noting the similarity and coverage between the two wind datasets, note the enhancement to the GOES-12 water vapor imagery (Figure 5.7) as compared to the GOES-8 water vapor imagery.
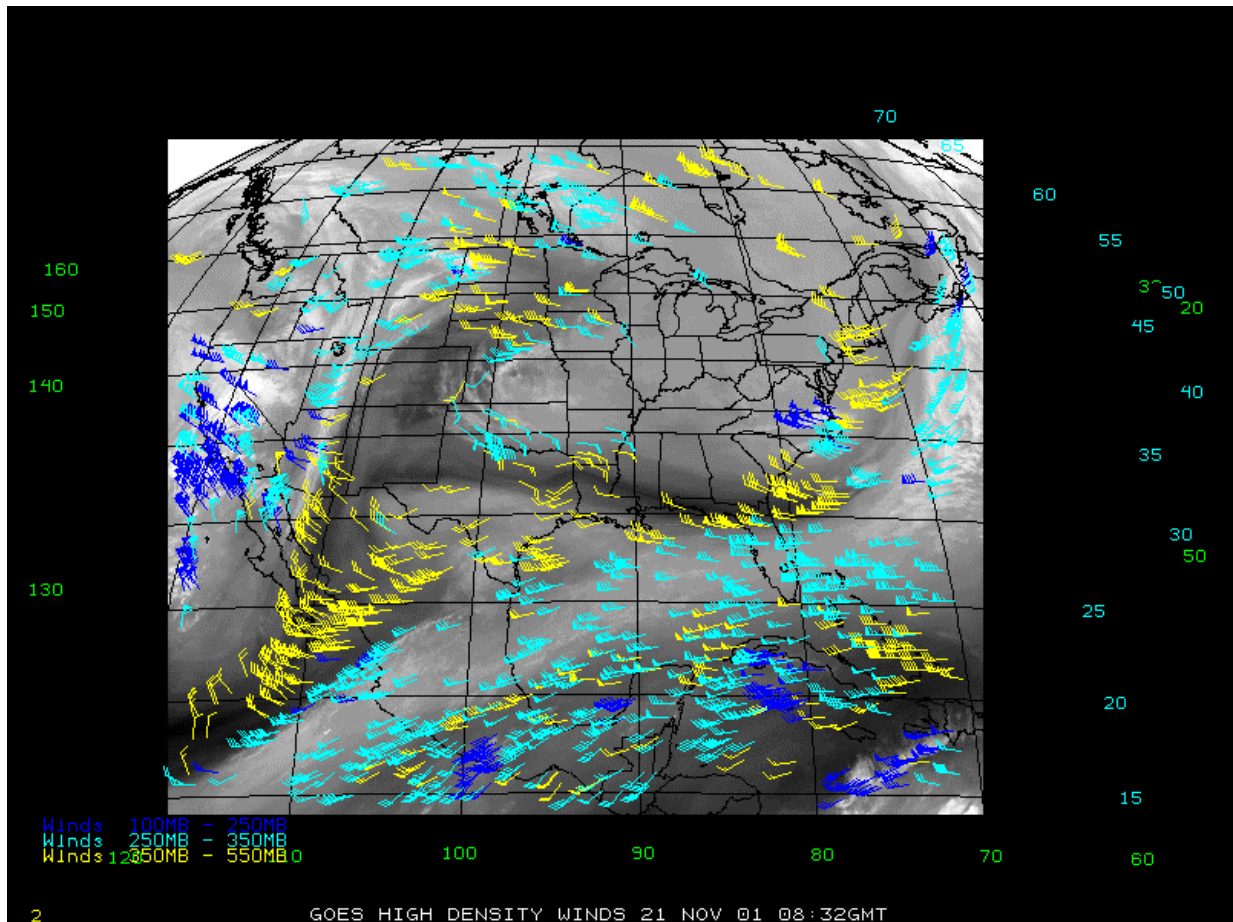
Figure 5.7: GOES-12 high-density water vapor winds.

An effort was made to investigate the state of the CO_2 slicing algorithm and how it was implemented with GOES-7. It was determined that a "cold sampling" procedure was used to obtain the observed 11 μm and 13.3 μm radiances used in the algorithm. In this procedure, a histogram of the 11 μm band radiances is constructed and the coldest 25% of the 11 μm pixels are determined. The coldest 11um radiances and accompanying 13.3 μm radiances are used to form an average radiance for each band that is then input to the CO_2 algorithm.

As an experiment, a new approach was attempted for arriving at a CO_2 solution. In this approach, a CO_2 solution was attempted at every single-field-of-view (SFOV) in the target scene and a histogram was constructed from all viable CO_2 solutions. Viable CO_2 solutions were those which passed several quality control tests which require that the target temperature be < 253K and cloud amount be > 10%. If at least 30% of the target scene contained viable CO_2 solutions, then a final CO_2 solution is determined by averaging the CO_2 pressures in the histogram bin containing the maximum frequency. This approach was run in parallel with the "cold-sampling" procedure described above (i.e., the control run) using GOES-12 imagery for the period 11–16 December 2001. The cloud-drift winds generated at 0000 UTC and 1200 UTC in both the control runs and the test runs were collocated in space and time with radiosonde winds and validation statistics were generated. An effort was made to ensure that the control and test satellite winds were collocated to the same radiosonde data so that an intercomparison could be

48

made between verification statistics generated for each. Table 5.2 shows these verification statistics. These statistics show a significant improvement in the average vector difference statistic by about 1 m/s, and an improvement in the speed bias by approximately 0.2 m/s.

Table 5.2: High-level (100-400 hPa) GOES-12 IR CO_2 Cloud-Drift Wind and Radiosonde Wind Difference Statistics. The column shows statistics for the CO_2 winds where the cold-sampling procedure was used. The second column shows statistics for the CO_2 winds where the single-field-of-view (SFOV) histogram approach was used.

	CO_2 Winds Cold-Sampling	CO_2 Winds SFOV Histogram
RMS Difference (m/s)	9.82	8.15
Normalized RMS (m/s)	0.27	0.23
Average Difference (m/s)	7.64	6.58
Standard Deviation (m/s)	6.17	4.80
Speed Bias (m/s)	0.51	0.33
Absolute Directional Diff (deg)	7.18	7.52
Speed (m/s)	37.40	36.47
Sample Size	72	72

The normalized root mean square (RMS) vector difference for the SFOV histogram approach of 0.23 m/s is an improvement over the normalized RMS vector difference of 0.27 m/s for the "cold-sampling" procedure. It is surmised that the SFOV histogram approach leads to more representative target height assignments since it accounts for the expected variability of the cloud heights at each pixel within the target scene. The "cold-sampling" procedure, on the other hand, favors the coldest pixels and then averages them, which may act to reduce any cloud height variability present in the target scene, and tends to assign cloud targets higher up in the atmosphere.

5.4.1   Comparison of CO_2 Heights and H_2O Intercept Heights

With GOES-12, the CO_2 slicing (SFOV-histogram approach) and the H_2O intercept algorithms are used to assign heights for semi-transparent or sub-pixel cloud tracers. Both methods are attempted for each cloud tracer. If both methods are successful in deriving a cloud height for a particular cloud tracer, then an inter-comparison of the heights derived from each method can be made. Table 5.3 presents results for about 1000 targets on 29 November 2001.

Table 5.3: CO_2 slicing and H_2O intercept cloud tracer height statistics using GOES-12 data on 29 November 2001.

	Mean cloud-top pressure (hPa)	Scatter with respect to mean (hPa)	Root Mean Square Deviation (hPa) with respect to:	
			CO_2 Slicing	H_2O Intercept
CO_2 Slicing	281	68	-	83
H_2O intercept	250	88	83	-

In the mean, the CO_2 height assignment is about 31 hPa lower in the atmosphere than the corresponding H_2O intercept height assignment. These results for this day are fairly representative and do agree with results from a similar comparison done by Nieman et al. 1993 where GOES-7 Visible Infrared Spin Scan Radiometer Atmospheric Sounder (VAS) data were used. In that study the authors noted that the CO_2 heights were about 30 hPa lower in the atmosphere than the corresponding H_2O intercept heights. The standard deviation in the heights of the clouds with respect to the mean heights is 68 hPa and 88 hPa for the CO_2 and H_2O intercept heights, respectively. The root mean square difference between the two height assignment methods is 83 hPa.

5.4.2   Verification of Winds: Assigned CO_2 Heights and H_2O Intercept Heights

Two sets of GOES-12 winds were generated, where the CO_2 slicing technique (SFOV-histogram approach) exclusively used for the first set, and the H_2O intercept technique was used exclusively for the second set. Each wind set was collocated to the same radiosonde data so that an intercomparison could be made between verification statistics generated for each. Table 5.4 shows these verification statistics.

Table 5.4: High-level (100-400 hPa) GOES-12 IR CO_2 Cloud-Drift Wind and Radiosonde Wind Difference Statistics. The first column shows statistics when the CO_2 slicing algorithm was used. The second column shows statistics when the H_2O intercept method was used.

	CO_2 Winds	H_2O Intercept Winds
RMS Difference (m/s)	7.62	7.90
Normalized RMS (m/s)	0.23	0.23
Average Difference (m/s)	5.24	5.50
Standard Deviation (m/s)	4.38	4.49
Speed Bias (m/s)	0.56	0.25
Absolute Directional Diff (deg)	7.07	7.26
Speed (m/s)	34.03	34.01
Sample Size	1783	1783

These statistics show comparable quality regardless of which height assignment is used. A slight reduction in RMS and mean vector difference is observed for the CO_2 winds, but these same winds exhibit a slightly larger speed bias. More work is needed to characterize these differences.

GOES-12 Imager results suggest that the H_2O/IR window intercept technique and the CO_2 slicing technique for inferring the heights of semi-transparent cloud elements produce similar results. The infrared window band technique consistently places the semi-transparent cloud elements too low in the atmosphere by 100 hPa or more; only in more opaque clouds does it perform adequately (Schreiner and Menzel 2002).

5.5   Clear Sky Brightness Temperature (CSBT)

A sample GOES-12 Imager Clear Sky Brightness Temperature cloud mask Image was generated and is shown in Figure 5.8. The GOES-12 Imager does not have the benefit of using the 12 µm band for use in cloud detection. The CSBT is used to initialize global numerical models.
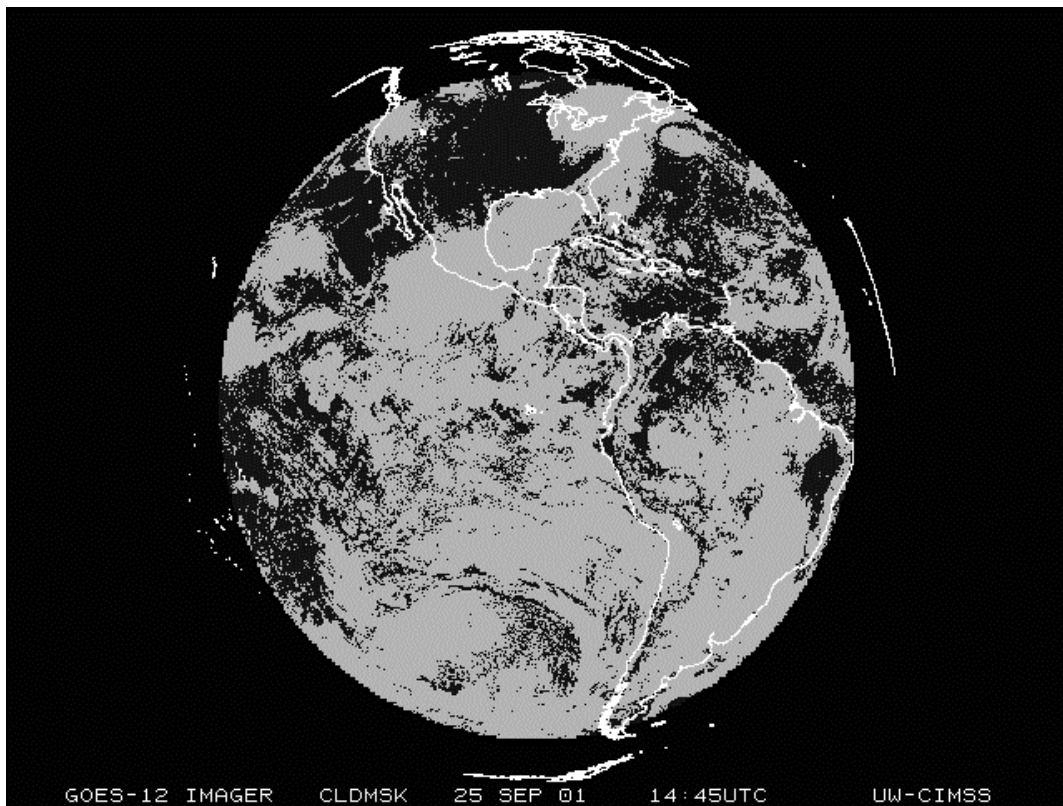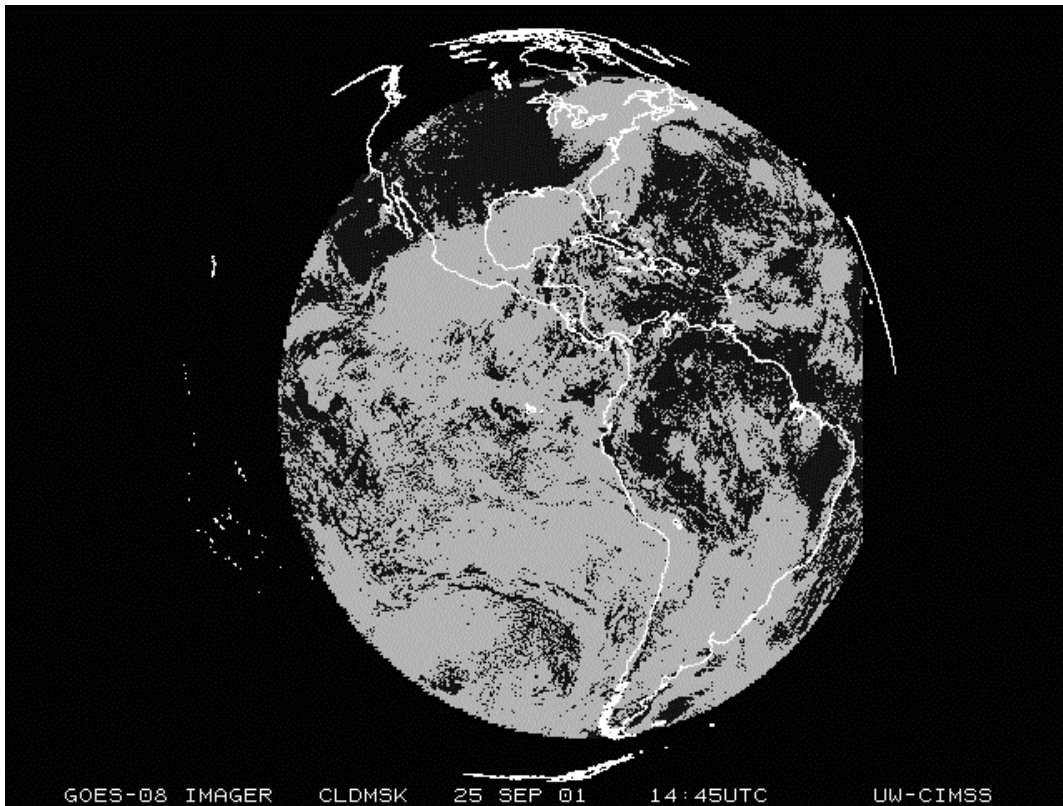
Figure 5.8: GOES-8 (top) and GOES-12 (bottom) Imager Clear-Sky Brightness Temperature cloud mask.

5.6   Sea Surface Temperature

The GOES-12 Imager lacks a 12 μm band, so the current focus is to derive GOES-12 sea surface temperatures (SST) at night. Past experience indicates that GOES-8 has a "nighttime" calibration problem. To prevent such problems from affecting the comparison, a 0545 UTC GOES-12 image from 16 November 2001 was chosen with the hope the GOES-8 calibration error would be small at this time. This is admittedly not the local midnight for GOES-10, but the "nighttime calibration problem" for GOES-10 is smaller and its SST is not used as extensively as that from GOES-8. For this image, pixels with SST from the operational product were identified, implying the pixels might be clear, because the operational SST product is a one-hour composite and cloud edges may appear to be different at different viewing angles. Therefore a very stringent cloud detection procedure was applied to those pixels, including a spatial coherence test and a spectral consistency test, which eliminated 90% of the pixels as not being clear. The operational GOES SST was then used as truth in regression with GOES-12 brightness temperatures. The first round resulted in a root-mean-square-difference (RMSD) of 0.56 K, relatively large because there were still a few outliers. Recursive regression removed 0.7% of the pixels that were outliers and reduced the RMSD to 0.41 K. All of the above were done to minimize cloud contamination in the regression data. The final regression formula is:

$$(1) \qquad G12\_SST = -1.23 + 1.0141 T_{3.9} + 0.152(T_{3.9} - T_{11}) + 0.345 ang$$

where all temperatures are in K, $ang = \sec(\theta)-1$, and θ is satellite zenith angle as viewed from the target. Separately, the GOES-12 SST has also been derived using simulated GOES-12 measurements produced via the MODTRAN forward radiative transfer model (Anderson et al. 1999):

$$(2) \qquad G12\_SST = (1.024 + 0.008 ang) T_{3.9} + (0.139 + 0.095 ang)(T_{3.9} - T_{11}) + 2.239 ang + 1.75$$

where all temperatures are in degrees C and *ang* is the same as before.

SST at 0145 UTC on 16 November 2001 was derived using (1) and is shown in Figure 5.9(a). For comparison, the operational GOES-8/10 SST at the same time is shown in Figure 5.9(b). The two are similar except that more cloud contamination is present in the GOES-12 SST. This is caused by the lack of the 12 μm band as a cloud detector on GOES-12. Proper application of the 13.3 μm band on GOES-12 is expected to alleviate this problem. Such an algorithm has been devised and tested with MODIS data but is not yet tuned for GOES-12 data. The GOES-12 SST using the simulation-based formula (2) (not shown) is on average 0.44 K cooler but otherwise similar. This is expected, because the simulation-based SST algorithm retrieves skin temperature, whereas the regression-based SST retrieval involves the mean of the bulk SST and variation of skin SST.
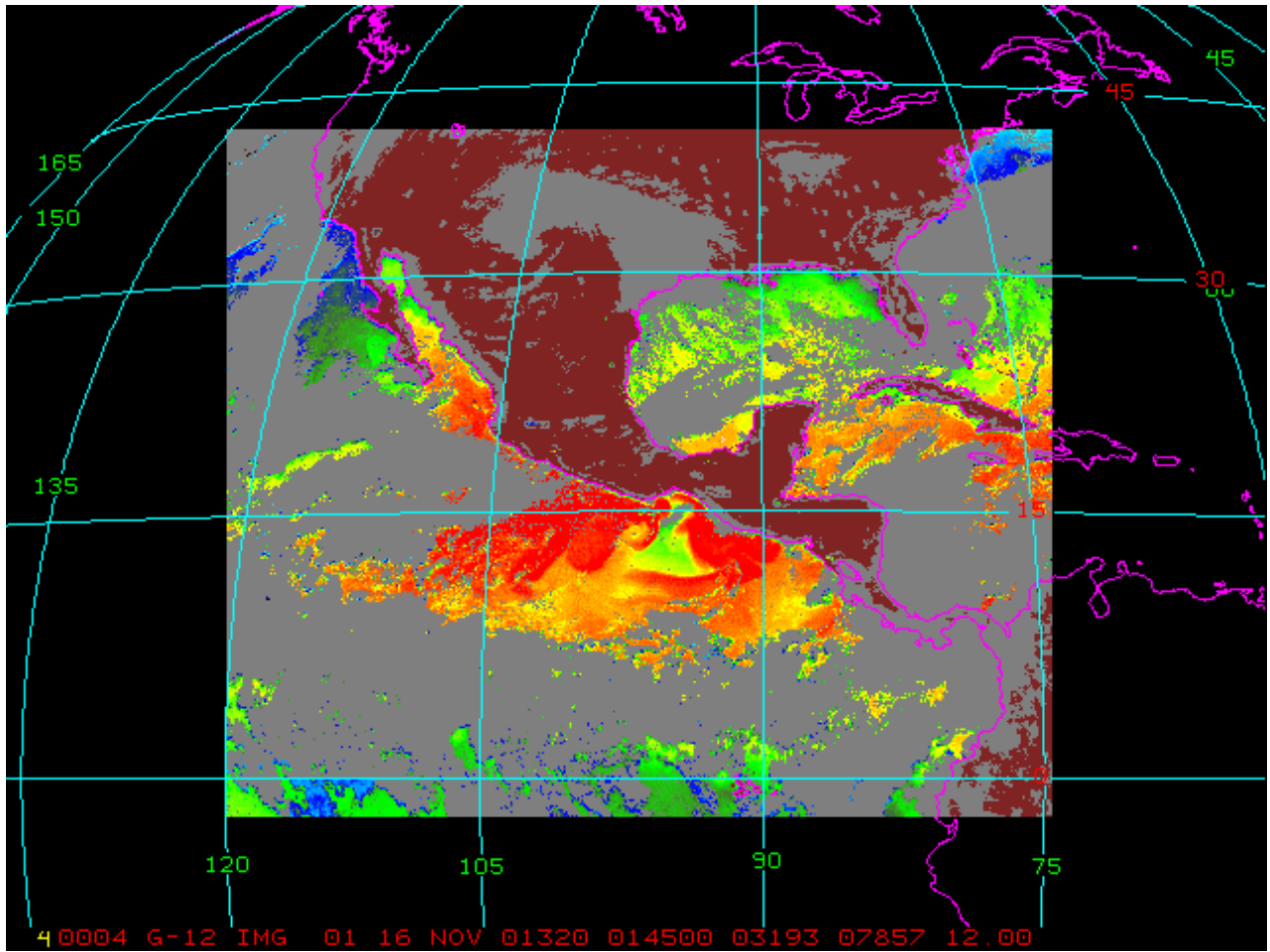
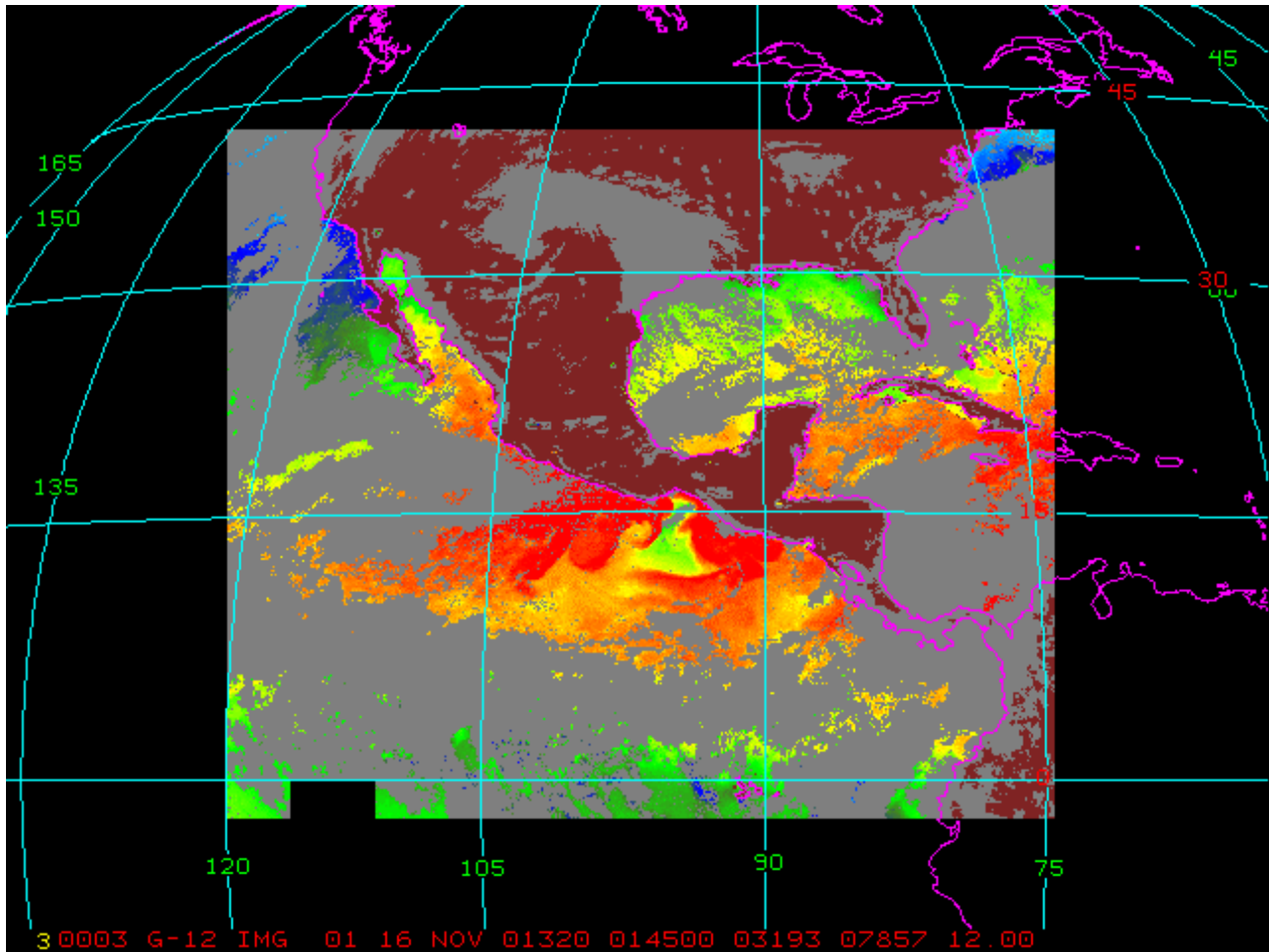Figure 5.9(a): Example of GOES-12 SST from 16 November 2001.

Figure 5.9(b): NOAA/NESDIS operational GOES-8/10 SST from 16 November 2001.

5.6.1   SST Algorithm Development

An initial radiative transfer model (RTM) GOES-12 algorithm with minimal cloud corrections and simple sun glint corrections (developed by the University of Edinburgh and ORAD) has been running since January 2002 in parallel with the operational GOES-8/10 SST algorithms. This initial algorithm was tested on GOES-12 data from November 2001. However, GOES-12 had calibration and registration offsets that were not discovered until after the algorithm was generated.

Processing runs applied the current GOES-12 algorithm form with sun glint and atmospheric corrections to GOES-8 operational data with the 12 μm channel excluded (hereinafter referred to as simulated GOES-12 data).   The match-up data base (MDB) covers the date range 12 September 2002 to 1 June 2003. The MDB used has been quality checked offline. The results of this study are shown in Table 5.5.

55

Table 5.5: Simulated GOES-12 results using simulated GOES-12 data

MDB Type	Bias (K)	Standard Deviation (K)
Day and Night	-0.30	0.77
Day	-0.01	0.91
Night	-0.47	0.62

The form of the GOES-12 initial algorithm is

(3)   a0 + a1*secZ-1 + a2*T3.9 + a3*T3.9*secZ-1 + a4*T11 + a5*T11*secZ-1

and is derived by regression against simulated clear-sky brightness temperatures using the MODTRAN radiative transfer model. The bias resulting from scattered solar radiation in the 3.9 μm channel is accounted for by

(4)   delta-SST = b0 + sec (SolZenAng)*sec (SatZenAng)*b1.

The scatter plots for day and night are shown in Figure 5.10.
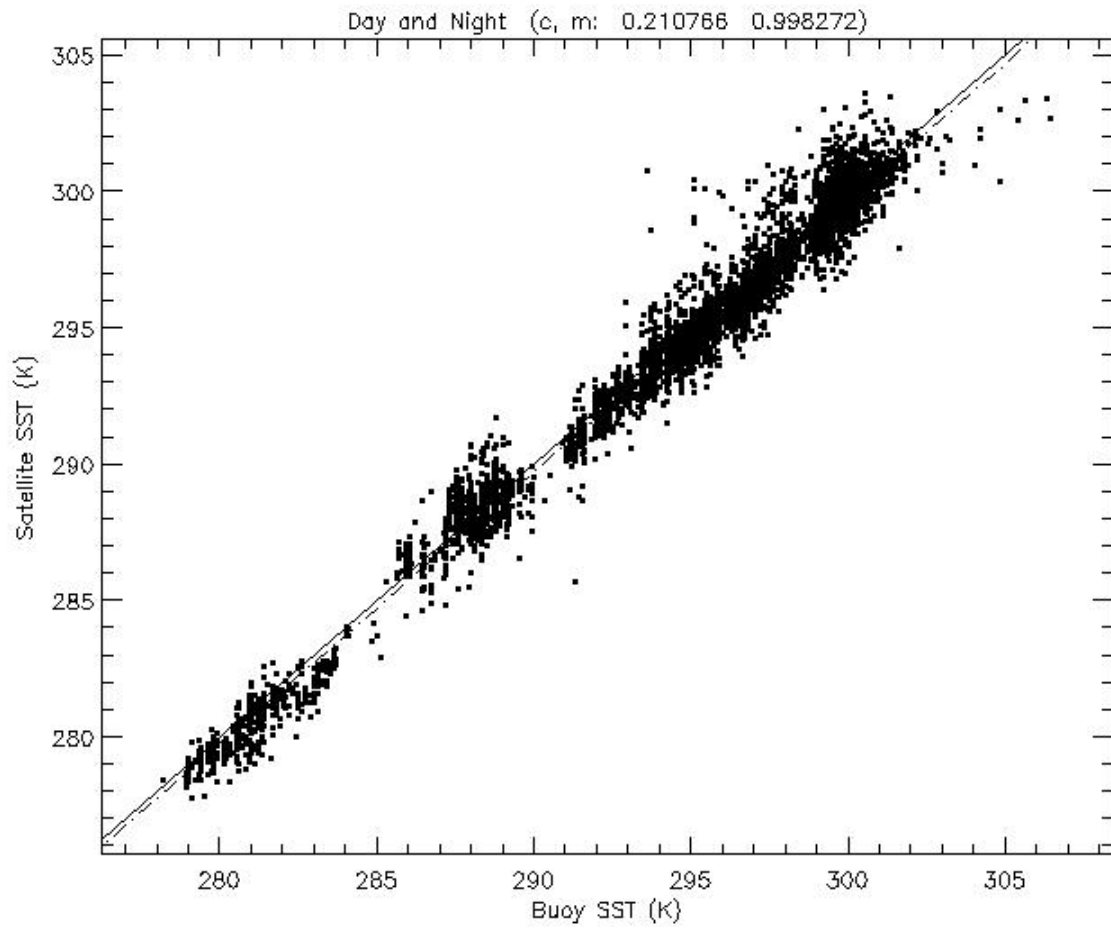
Figure 5.10a: Simulated GOES-12 SST vs. buoy SST for day and night.
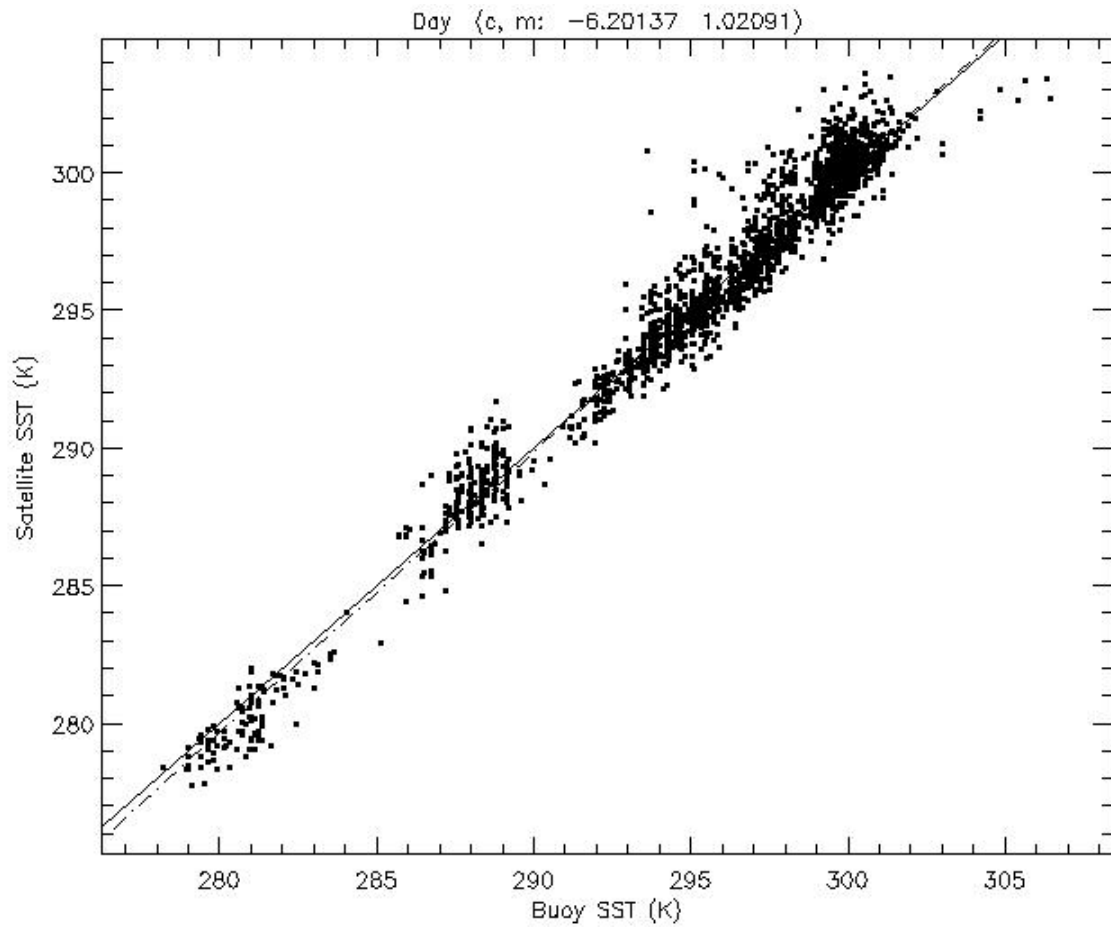
Figure 5.10b: Simulated GOES-12 SST vs. buoy SST day
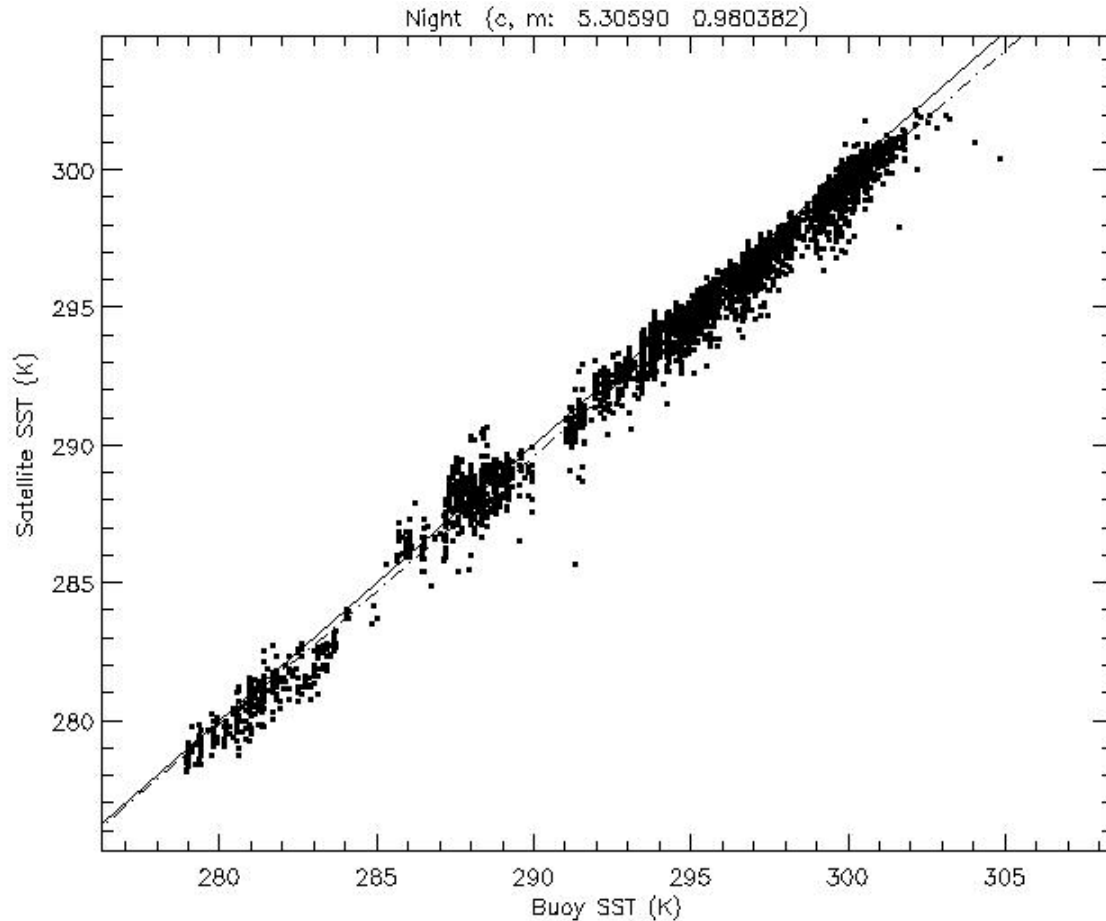
Figure 5.10c: Simulated GOES-12 SST vs. buoy SST

This GOES-12 algorithm is being transitioned into operations in cooperation with the University of Edinburgh. This will involve implementation of advanced techniques for cloud clearing, aerosol correction and sun glint contamination.

5.7   Fire Detection

Basic fire detection relies primarily on 3.9 μm (band-2) data from the GOES Imager. This provides the basis for locating the fire and other information aids in estimating the sub-pixel fire size and temperature. The number of fires that can be successfully detected and characterized is related to the upper limit of the observed brightness temperature in the 3.9 μm band. The saturation temperature of the 3.9 μm band limits the number of fires that can be detected and processed. The higher the saturation temperature, the greater the opportunity to identify and estimate sub-pixel fire size and temperature. Low saturation temperatures can result in the inability to distinguish fires from hot background in places where the observed brightness temperature meets or exceeds the saturation temperature.

GOES-12 has a saturation temperature (approximately 336 K) similar to both GOES-8 and GOES-12. The sub-satellite point of GOES-8 is at the equator and 75°W while for GOES-12

59

during the Science Test was at the equator and 90°W. Therefore, fire pixels observed by both instruments in the Mato Grosso region of Brazil (approximately 12°S and 55°W) show some variation in brightness temperature with GOES-8 tending to saturate more often than GOES-12 in South America as demonstrated in comparisons performed at CIMSS (not shown). Three locations of active fires were selected for comparison at 1745 UTC on 2 October 2001. Even with satellite view angle differences of 15º, the comparisons display relatively good agreement in the location and number of fire pixels. In all three examples, differences in clear-sky non-fire pixels were typically less than 2 K. In the first example the fire intensity was so great, that it easily saturated both GOES-8 and GOES-12. The GOES-8 observations of the fire activity in the first example showed the fire's impact on more scan lines, which was most likely due to respective viewing geometry. The other two examples also showed the impact of the satellite view angle. In example 2, the fire was just hot enough to saturate the GOES-8 3.9 µm band, but not hot enough to saturate GOES-12. In the third example, both instruments saturated, but there were large differences in several pixels, which was probably due to view angle differences and fire intensity.

A comparison of the GOES-10 to GOES-12 3.9 µm brightness temperatures was performed for a hot spot in the state of California at 37.5°N, 121.5°W (not shown). This example illustrated the need for elevated saturation brightness temperatures in the shortwave infrared window of the GOES Imager. The satellite viewing angles were nearly 9° different, with GOES-10 viewing the fire from the west and GOES-12 viewing the fire from the east through different atmospheres. The GOES-10 and GOES-12 background brightness temperatures surrounding the fires were typically within 2 K. GOES-12 did not immediately record an increased brightness temperature at the western edge of the fire pixels. This was likely due to the larger satellite zenith angle of GOES-12 in that region. The fire saturated the GOES-10 3.9 µm Imager band at 321.5 K, while the GOES-12 saturated at 336.3 K. As a rule, the reduced saturation brightness temperature in the GOES-10 3.9 µm band hinders fire identification in the Western U.S. and results in an inability to characterize sub-pixel fire activity for most wildfires in North America.

Preliminary indications are that GOES-12 is performing comparably to GOES-8 and much better than GOES-10 insofar as fire detection is concerned.

The Biomass Burning team at CIMSS currently produces fire products for GOES-10/12 covering North and South America. These data can be viewed at the Wildfire Automated Biomass Burning Algorithm page (http://cimss.ssec.wisc.edu/goes/burn/wfabba.html).

5.8   Volcanic Ash Detection

MODIS data for two volcanoes (Popocatepetl near Mexico City and Cleveland in the Aleutian Islands) were used to simulate the impact of changes that will occur in spectral bands between current GOES-8/11 and GOES-12 imagery. The change from the 12.0 : m band to a 13.3 : m band on GOES-12 was made to improve cloud height determinations. However, the change in bands will have a potential negative impact on image products that are heavily utilized for volcanic ash detection. Image products generated from the three GOES infrared bands, with the 13.3 : m band substituted for the 12.0 : m band, indicated that volcanic ash can still be detected, but with diminished ability, especially for diffuse ash. For both day and night cases the

increased contamination by clouds leads to increased chances of false ash detection for the cases examined. See Hillger and Clark (2002) for complete details of this study.

GOES-8 Sounder data were also evaluated for two weak-to-moderate eruptions to estimate possible negative effects resulting from loss of the 12 µm Split Window IR (SWIR) band. Principal Component Images (PCIs) with and without the SWIR were compared subjectively using pattern recognition techniques, and objectively by means of a "false alarm" parameter (Ellrod 2001). GOES Sounder data were also evaluated to assess any potential contributions from the new 13.3 µm Imager band. During periods of daylight, there was little apparent difference in the quality of IR detection without the SWIR, likely due to the reflectance peak of silicate ash near 3.9 µm. This was especially true during periods when the ash cloud was opaque, rendering the Split Window technique less effective. At night, the ash detection capability appeared to be significantly worse, due to increased ambiguity with clouds or surface features. The effects of this degradation on aviation operations could be an occasional increase in the area of analyzed ash coverage to err on the side of safety, resulting in somewhat longer route diversions. Otherwise, it is believed that with the aid of image animation, an analyst should be able to track volcanic ash clouds sequentially to determine approximate locations.

For long-lasting ash clouds caused by major eruptions, there is the risk of "losing" the ash cloud, especially where there is a significant amount of high-level cirrus cloud cover. The new 13.3 µm IR band on GOES-12 appears to be capable of distinguishing ash from cirrus clouds, but not from low-level water droplet clouds and some surface features. The scatter plot in Figure 5.11 shows 11 µm – 13.3 µm Brightness Temperature Differences (BTDs) from the GOES-8 Sounder for an ash cloud from Popocatepetl volcano on the night of 23 January 2001. For a given IR temperature, there are significant differences in the BTDs for cirrus versus ash, allowing differentiation.
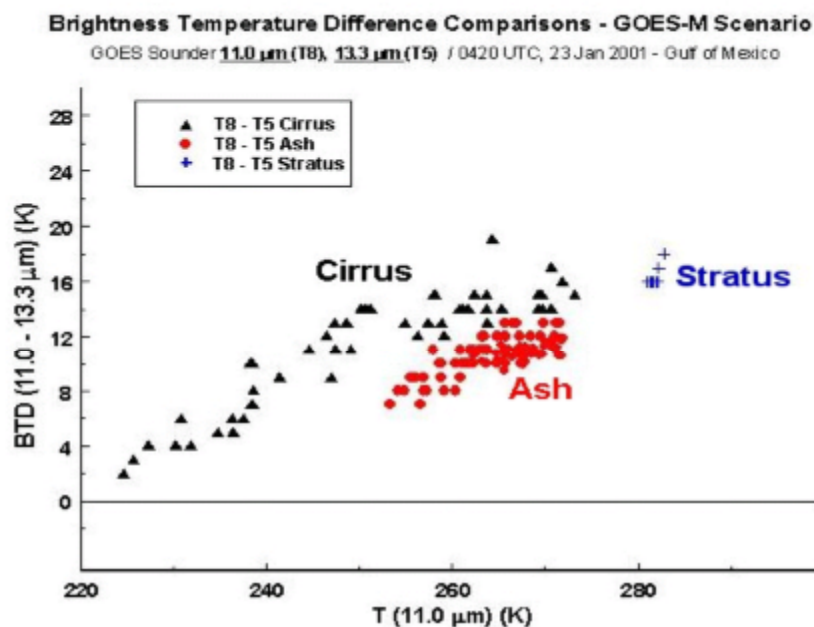

Figure 5.11: Scatter plot of Brightness Temperature Differences (BTDs) from the GOES-8 Sounder for an ash cloud from Popocatepetl volcano on 23 January 2001 at 0420 UTC (night).

During the GOES-12 Science Test, the only opportunity to evaluate volcanic ash detection capability was on 9 October 2001, when a small emission of ash from Popocatepetl, near Mexico City, was observed. A PCI based on the 3.9 μm, 11 μm, and 12 μm IR bands from GOES-8 was compared to a similar image based on the 3.9 μm, 11 μm, and 13.3 μm bands from GOES-12 at 1445 UTC (Figure 5.12). While the small ash cloud stands out well in both images, the GOES-8 image provides the best contrast, while the GOES-12 image appears to slightly underestimate the area coverage of the cloud without contribution from the 12.0 μm band. Thus, while it appears that analysts will still be able to detect and track volcanic ash clouds using GOES-12, the capability will be degraded, especially during nighttime hours.
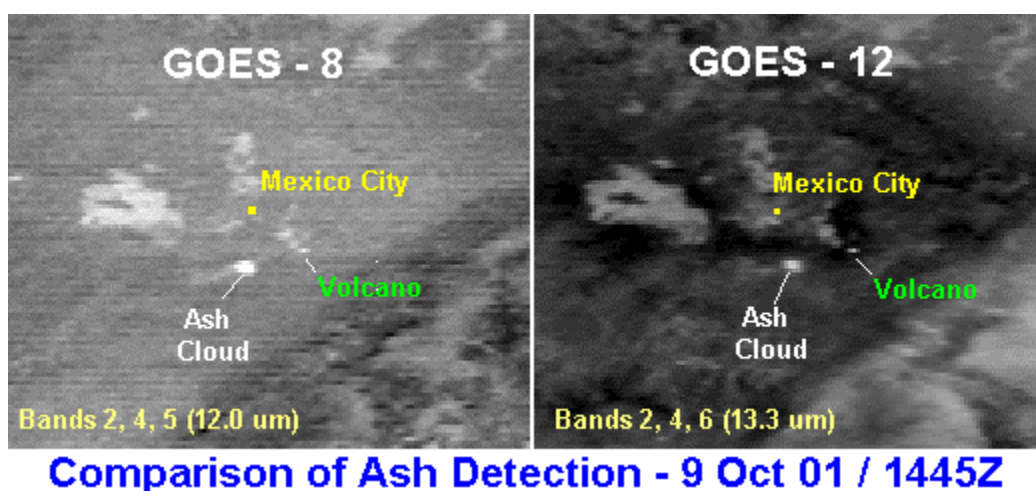
Figure 5.12: A Principal Component Image (PCI) based on the 3.9 μm, 11 μm, and 12 μm IR bands from GOES-8 was compared to a similar image based on the 3.9 μm, 11 μm, and 13.3 μm bands from GOES-12 at 1445 UTC.

6.0   Other accomplishments with GOES-12

6.1   Update of Albedo Software for GOES-12

The software to generate both the shortwave albedo and day/night visible/shortwave albedo products has been updated to include calibration coefficients for GOES-12. Because of changes in the GVAR stream starting with GOES-12 the software had to be modified more significantly than previous upgrades such as for GOES-11 where there was no change in the GVAR. Calibration data for the upgrade were obtained from the Office of Satellite Operations GOES Calibration at: http://www.oso.noaa.gov/goes/goes-calibration/index.htm

6.2   Super Rapid Scan Operations (SRSO) of Severe Weather

One-minute interval scans with GOES-12 were requested and archived at CIRA for a tornado outbreak that occurred on 9 October 2001. Data were collected from 1800 UTC through 0100

UTC, spanning the entire event from the pre-storm environment through the time of all tornado reports. A satellite interpretation discussion was made for the event and can be fount at: http://www.cira.colostate.edu/ramm/picoday/011010/011010.html

6.3   NASA E-Theatre Premiere of GOES-12 Science Test 1-minute Imagery

Collaboration between NOAA/CIRA and the NASA Visualization and Analysis Laboratory has resulted in a High Definition Television (HDTV) version of the 9 October 2001 1-minute imagery sequence. The segment was an anaglyph (red/green) stereo version of a line of tornadic thunderstorms in Kansas and Nebraska. The imagery was presented to two sold-out IMAX theatre audiences at the Science Museum of Minnesota in St. Paul MN. In addition, NASA has requested more GOES-12 imagery, including examples of the 4 km water vapor imagery for the tornadic storm case.   For further information, see the NASA E-theatre Web page at: http://etheater.gsfc.nasa.gov/index.html

Acknowledgments

References

Anderson, G.P. and Co-authors, 1999: MODTRAN4: Radiative Transfer Modeling for Remote Sensing. *Optics in Atmospheric Propagation and Adaptive Systems III*, **3866**, 2-10.

Daniels, J.M., T.J. Schmit, and D.W. Hillger, 2001: GOES-11 Imager and Sounder Radiance and Product Validations for the GOES-11 Science Test, *NOAA Technical Report NESDIS 103*, (August), 49 pp.

Ellrod, G.P., 2001: Loss of the 12.0 μm "Split Window" Band on GOES-M: Impacts on Volcanic Ash Detection, *11th Conf. Sat. Meteor. Ocean.*, 15-18 October, Madison WI, 61-64.

Hillger, D.W., 2002: Changes in the GOES-12 Imager, *CIRA Newsletter, 17,* spring, 13-14.

Hillger, D.W., and J.D. Clark, 2002: Principal Component Image analysis of MODIS for volcanic ash, Part-2: Simulations of current GOES and GOES-M Imagers, *J. Appl. Meteor.*, **41**, 1003-1010

Hillger, D.W., and T.H. Vonder Haar, 1988: Estimating Noise Levels of Remotely Sensed Measurements from Satellites Using Spatial Structure Analysis. *J. Atmos. Oceanic Technol.*, **5**, 206-214.

Ma, Xia L., T.J. Schmit, and W.L. Smith, 1999: A nonlinear physical retrieval algorithm—its application to the GOES-8/9 Sounder. *J. Appl. Meteor.*, **38**, 501-513.

Menzel, W. P., and J. F. W. Purdom, 1994: Introducing GOES-I: The first of a new generation of Geostationary Operational Environmental Satellites. *Bull. Amer. Meteor. Soc.,* **75**, 757-781.

Menzel, W.P., W.L. Smith, and T.R. Stewart, 1983: Improved cloud motion vector and altitude assignment using VAS. *J. Climate Appl. Meteor.*, **22,** 377-384.

Menzel, W.P., F.C. Holt, T.J. Schmit, R.M. Aune, G.S. Wade, D.G. Gray, and A.J. Schreiner, 1998: Application of GOES-8/9 Soundings to weather forecasting and nowcasting. *Bull. Amer. Meteor. Soc.,* **79**, 2059-2078.

Nieman, S., J. Schmetz, and W.P. Menzel, 1993: A comparison of several techniques to assign heights to cloud tracers, *J. Appl. Meteor.,* **32**, 1559-1568.

Schmetz, J., and K. Holmlund, 1992: Operational cloud motion winds from Meteosat and the use of cirrus clouds as tracers. *Adv. Space Res.*, **12**, 95-104.

Schmit, T.J., E.M. Prins, A.J. Schreiner, and J.J. Gurka, 2001: Introducing the GOES-M Imager. *Nat. Wea. Dig.*, **25**(3/4).

Schmit, T.J., W.F. Feltz, W.P. Menzel, J. Jung, A.P. Noel, J.N. Heil, J.P. Nelson III, G.S. Wade, 2002: Validation and Use of GOES Sounder Moisture Information. *Wea. Forecasting,* **17**, 139-154.

Schreiner, A.J. and W.P. Menzel, 2002: Comparison of Three Cloud Height Techniques using GOES-12 Imager Data. Reprints, *6th Int. Winds Workshop*, Madison WI.

Weinreb, M.P., M. Jamison, N. Fulton, Y. Chen, J.X. Johnson, J. Bremer, C. Smith, and J. Baucom, 1997: Operational calibration of Geostationary Operational Environmental Satellite-8 and -9 Imagers and Sounders. *App. Opt.*, **36**, 6895-6904.

Appendix A: Web Sites Related to the GOES-12 Science Test

http://www.cira.colostate.edu/ramm/goesm/test_schedules.htm -- GOES-12 Science Test schedules

http://www.cira.colostate.edu/ramm/goesm/test_results.htm -- RAMMT/CIRA Contributions to the GOES-12 Science Test results

http://www.cira.colostate.edu/ramm/goesm/testing_philosophy_goals.htm -- GOES-12 testing philosophy

http://www.cira.colostate.edu/RAMM/rmsdsol/goes12main.html -- RAMSDIS OnLine (ROL) GOES-12 Science Test imagery (live during the test period)

http://www.cira.colostate.edu/Special/CurrWx/wxgoes12.htm -- CIRA GOES-12 current imagery

http://www.cira.colostate.edu/Infrastructure/Internet/GOES12Over.htm -- CIRA GOES-12 jpeg archive

http://www.cira.colostate.edu/ramm/PICODAY/011010/011010.html -- CIRA Satellite Interpretation Discussion of GOES-12 Super Rapid Scan Operations (SRSO) during the 9 October 2001 Great Plains tornado event

http://www.cira.colostate.edu/RAMM/PICODAY/011119/011119.html -- CIRA Satellite Interpretation Discussion of the two significant changes that have made to the GOES-12 Imager

http://cimss.ssec.wisc.edu/goes/g12_report/ -- On-line CIMSS GOES-12 report

http://cimss.ssec.wisc.edu/goes/realtime/g12/g12realtime.html -- CIMSS realtime GOES-12 page

http://cimss.ssec.wisc.edu/tropic/ -- CIMSS tropical home page

http://cimss.ssec.wisc.edu/goes/burn/abba.html -- CIMSS home page for biomass burning

http://cimss.ssec.wisc.edu/goes/realtime/realtime.html -- CIMSS realtime Sounder home page

http://www.ssec.wisc.edu/software/mcidas.html -- McIDAS home page

http://www.oso.noaa.gov/goes/goes-calibration/change-channels.htm -- Change of bands on Imagers beginning with GOES-12

http://www.oso.noaa.gov/goes/goes-calibration/index.htm -- GOES calibration

Appendix B: Acronyms Used in this Report

ASOS   Automated Surface Observing System

ASPT   Advanced Satellite Products Team

AVHRR   Advanced Very High Resolution Radiometer

AVIRIS   Airborne Visible InfraRed Imaging Spectrometer

BTD   Brightness Temperature Difference

CART   Cloud And Radiation Testbed

CICS   Cooperative Institute for Climate Studies

CIMSS   Cooperative Institute for Meteorological Satellite Studies

CIRA   Cooperative Institute for Research in the Atmosphere

CONUS   Continental United States

CSBT   Clear Sky Brightness Temperature

DPI   Derived Product Image

ECA   Effective Cloud Amount

FOV   Field Of View

FPDT   Forecast Products Development Team

GOES   Geostationary Operational Environmental Satellite

GVAR   GOES Variable (data format)

HDTV   High Definition Television

HIRS   High-resolution InfraRed Sounder

hPa   Hectopascals (equivalent to millibars)

IGFOV   Instantaneous Geometric Field Of View

IR   InfraRed

LI   Lifted Index

McIDAS	Man-Computer Interactive Data Access System
MDB	Match-up Data Base
MODIS	Moderate Resolution Imaging Spectroradiometer
NASA	National Aeronautics and Space Administration
NESDIS	National Environmental Satellite, Data, and Information Service
NOAA	National Oceanic and Atmospheric Administration
ORA	Office of Research and Applications
ORAD	Ocean Research and Applications Division
OSDPD	Office of Satellite Data Processing and Distribution
OSO	Office of Satellite Operations
PCI	Principal Component Image
PLOD	Pressure-Layer Optical Depth
RAMMT	Regional and Mesoscale Meteorology Team
RAMSDIS	RAMM Advanced Meteorological Satellite Demonstration and Interpretation System
RMS	Root Mean Square
RMSD	RMS Difference
RSO	Rapid Scan Operations
RT	Real Time
RTTOVS	Real Time TIROS Operational Vertical Sounder
RTM	Radiative Transfer Model
SAB	Satellite Analysis Branch
SCP	Satellite Cloud Products
SFOV	Single Field Of View
SIT	Soundings and Instrument Team

SOCC	Satellite Operations Control Center
SPEC	Specifications
SRF	Spectral Response Function
SRSO	Super Rapid Scan Operations
SSD	Satellite Services Division
SSEC	Space Science and Engineering Center
SSR	Sampled Subpoint Resolution
SST	Sea Surface Temperature
SWIR	Split-Window InfraRed
TIROS	Television and Infrared Radiation Observation Satellite
TOVS	TIROS Operational Vertical Sounder
TPW	Total Precipitable Water
UTC	Coordinated Universal Time
VAS	VISSR Atmospheric Sounder
VISSR	Visible and Infrared Spin-Scan Radiometer
WV	Water Vapor

NOAA SCIENTIFIC AND TECHNICAL PUBLICATIONS

The National Oceanic and Atmospheric Administration was established as part of the Department of Commerce on October 3, 1970. The mission responsibilities of NOAA are to assess the socioeconomic impact of natural and technological changes in the environment and to monitor and predict the state of the solid Earth, the oceans and their living resources, the atmosphere, and the space environment of the Earth.

The major components of NOAA regularly produce various types of scientific and technical information in the following types of publications:

PROFESSIONAL PAPERS - Important definitive research results, major techniques, and special investigations.

CONTRACT AND GRANT REPORTS - Reports prepared by contractors or grantees under NOAA sponsorship.

ATLAS - Presentation of analyzed data generally in the form of maps showing distribution of rainfall, chemical and physical conditions of oceans and atmosphere, distribution of fishes and marine mammals, ionospheric conditions, etc.

TECHNICAL SERVICE PUBLICATIONS - Reports containing data, observations, instructions, etc. A partial listing includes data serials; prediction and outlook periodicals; technical manuals, training papers, planning reports, and information serials; and miscellaneous technical publications.

TECHNICAL REPORTS - Journal quality with extensive details, mathematical developments, or data listings.

TECHNICAL MEMORANDUMS - Reports of preliminary, partial, or negative research or technology results, interim instructions, and the like.

U.S. DEPARTMENT OF COMMERCE
National Oceanic and Atmospheric Administration
National Environmental Satellite, Data, and Information Service
Washington, D.C. 20233